Coordination Chemistry Reviews 254 (2010) 1661–1685

Contents lists available at ScienceDirect

Coordination Chemistry Reviews

journal homepage: www.elsevier.com/locate/ccr

Review

Preparations and applications of synthetic linked azamacrocycle ligands and complexes

J. Cody Timmons, Timothy J. Hubin*

Department of Chemistry and Physics, Southwestern Oklahoma State University, 100 Campus Drive, Weatherford, OK 73096, USA

Contents

ARTICLE INFO

Article history:
Received 19 June 2009
Accepted 16 September 2009
Available online 23 September 2009

Keywords:
Azamacrocycle
Linked azamacrocycle
Binucleating
Ligand synthesis

ABSTRACT

Covalently linked azamacrocycles have been known for several decades, but only a modest number of these ligands and their complexes had been described prior to 2000. Since that time, a number of new synthetic methods for their preparation have been discovered, yielding a growing collection of these interesting ligands. Additionally, the number of uses to which these ligands and their metal complexes have been applied has expanded. In this review, the important synthetic methods yielding linked azamacrocycles will be outlined, and their applications will be discussed.

1. Introduction

Inspired by the natural porphyrin and corrin rings (Fig. 1), chemists have produced synthetic azamacrocycles intentionally and in high yields for only about 50 years. Predated only by the phthalocyanines (Fig. 1) [1], an important yet limited early family of synthetic macrocycles with a strong resemblance to the natural sys-

* Corresponding author. Tel.: +1 580 774 3026; fax: +1 580 774 3115.
E-mail address: tim.hubin@swosu.edu (T.J. Hubin).

0010-8545/$ – see front matter © 2009 Elsevier B.V. All rights reserved.
doi:10.1016/j.ccr.2009.09.018

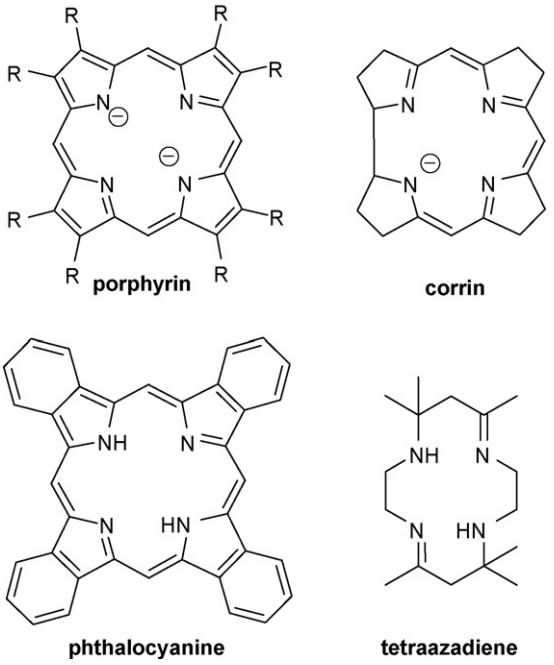

Fig. 1. Naturally occurring (top) and early synthetic (bottom) azamacrocycles.

tems, azamacrocycles in the initial form of tetraazadienes appeared in 1960 (Fig. 1) [2]. This discovery was made several years prior to the crown ethers [3], and synthetic azamacrocycles, crucially aided by the development of metal ion template synthetic routes [2b,4], rapidly developed into a staple for coordination chemistry. In the intervening years, clever synthetic chemists have continued to produce more, and more complex, azamacrocycles with important applications alone and/or in their metal ion complexes [5].

One simple to conceive, yet potentially difficult to carry out, alteration to an azamacrocycle is to join it with another. Architectures produced by joining rings (Fig. 2) include (1) fused ring systems—those in which one or more atom belongs to two or more of the rings; (2) mechanically interlocked multi-ring systems, commonly called catenanes; and (3) linked ring systems—here defined as those not mechanically bonded and having no atoms belonging to more than one macrocyclic ring (**7**).

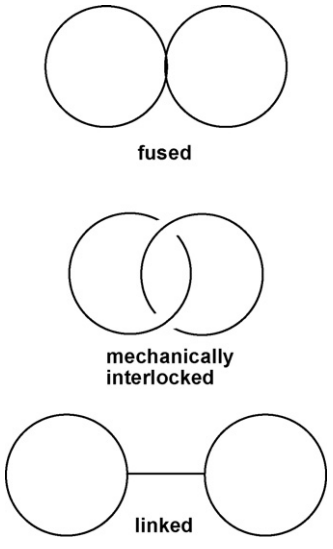

Fig. 2. Types of architectures produced by joining rings. This review will focus on the linked systems.

This review will focus on linked synthetic azamacrocycles (where all donor atoms are nitrogen), concentrating on systems published since the year 2000. Significant progress has been made concerning this subset of linked macrocycles since that time, with no major reviews appearing that we are aware of. Several previous reviews on linked macrocycles were published about that time [6], with two specifically targeting the linked azamacrocycles [7]. Our goal is to update the progress in linked azamacrocycles since then. We will first focus on new synthetic methods (and new examples of old methods) used to produce linked azamacrocycles. We will then turn our attention to the application of linked azamacrocycles to specific problems, beginning with applications of the free ligands and then moving to the major applications of their metal complexes. Due to space constraints, the complexation of metal ions to linked azamacrocycles and the subsequent physical and chemical characterization of those complexes will not be considered a separate "application" for the purposes of this review. The literature since 2000 includes a large number of such studies [8] and would be an excellent topic for review. However, we have chosen to focus this part of the review on instances where these complexes are applied to other chemical problems, as a way to highlight the importance of linked azamacrocycles and their complexes to the broader field of chemistry.

2. Synthetic methods for linking azamacrocycles

2.1. N–N linking

Classically, the nitrogen–nitrogen (N–N) linking of azamacrocycles has proved to be the most common and practical form of linkage due to the reactivity of the nitrogen functionality. However, controlling the mono N–N linkage has often posed a challenge in the presence of the multiple reactive nitrogens. In recent years, several innovative methods for the synthesis of these linked azamacrocycles have been described. These methodologies have most commonly exploited the nucleophilicity of the amine functionality, either as a donor in displacement reactions or as a Schiff base coupling partner.

2.1.1. Bis-aminal strategies

One such broad-scoped methodology was reported by Handel and co-workers in 2001 [9]. The authors described the reactivity of bis-aminals formed by the condensation of tetraazamacrocycles (e.g. cyclen, cyclam, homocyclam) with glyoxal [10]. The alkylation of these bis-aminals to form the corresponding ammonium salts was found to be highly dependent on proper solvent selection. When dihalides were employed as electrophiles, exclusive mono-alkylation was observed in either THF or benzene. The success of this selectivity can be attributed to the low solubility and resulting precipitation of the initially formed ammonium salt in the stated reaction media. However, these mono-ammonium salts were found to be sufficiently soluble in acetonitrile to allow for subsequent reactions. Alkylation with a second equivalent of bis-aminal resulted in the formation of the corresponding N–N linked bis-macrocycle, thus allowing for the formation of either symmetrical or unsymmetrical bis-macrocyclic ligands (Scheme 1). Alternatively, the direct formation of symmetrical bis-macrocycles was achieved in a one-pot process using acetonitrile as the solvent and with proper choice of stoichiometry. The authors found that the bis-ammonium macrocycles could be neutralized by transamination using hydroxylamine.

It was also found that the synthesis of N–N linked macrocycles with pendant arms was possible with the bis-aminal methodology. Exploiting a Gabriel-type synthesis, the authors alkylated cyclen with bromoalkyl phthalimide derivatives (Scheme 2). By control-

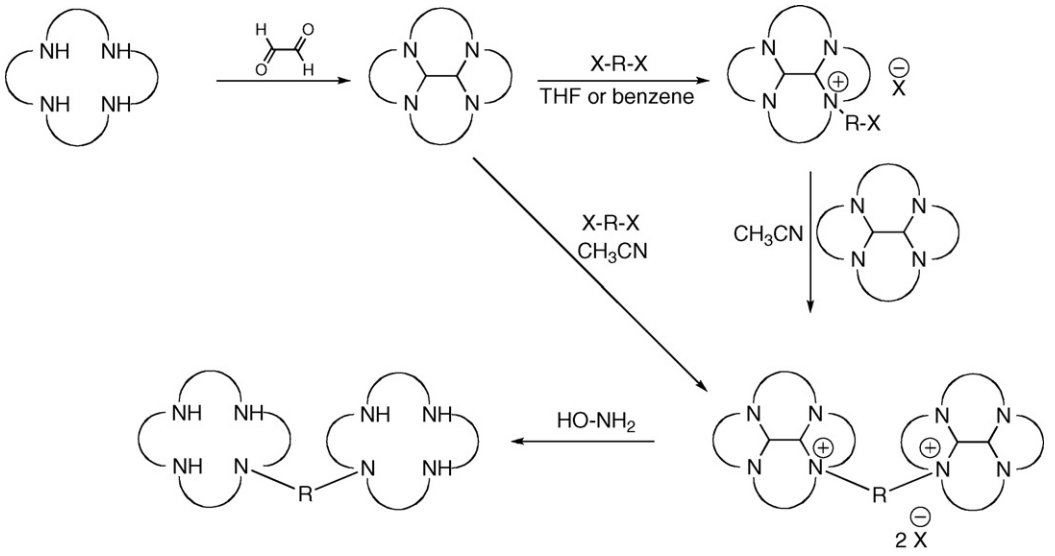

Scheme 1.

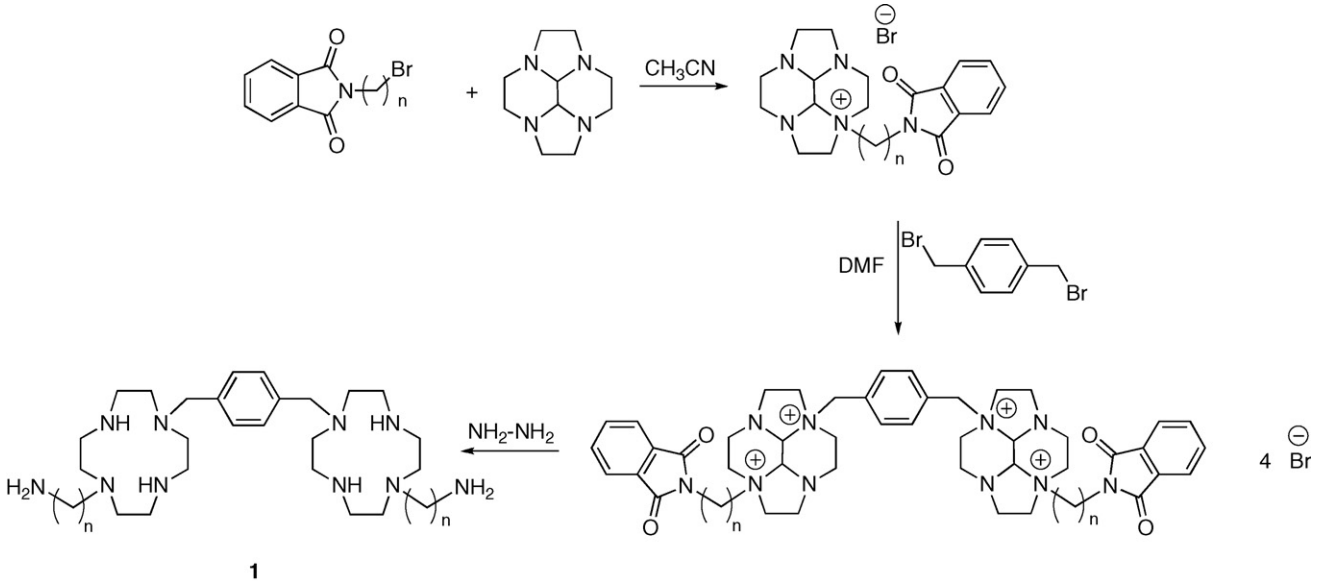

Scheme 2.

ling stoichiometry and with the use of acetonitrile as a solvent, the authors realized selective mono-addition. Subsequent treatment with *p*-xylyl dibromide in DMF affected the desired linkage to afford the bis-macrocyclic aminal derivative. Final treatment with hydrazine liberated the fully free decaaza bis-macrocycle **1**.

The above synthesis illustrates a key defining feature of the bis-aminal strategy. Notably, the alkylation steps occur in a selective N1–N3 regiochemistry. The authors explored this high selectivity by variable temperature NMR studies and by performing calculations at the AM1 level of theory. It was found that bis-aminals of this nature exhibit a *cis* configuration about the two-carbon bridge (Fig. 1). Arising from this relatively rigid structural feature is the necessity for a bowl-like folded geometry with convex and concave faces. The lone pairs on N1 and N3 point towards the convex face of the macrocycle, making them more nucleophilic than the lone pairs on N2 and N4, which point towards the interior concave face. Thus alkylation preferentially occurs at N1 and N3 (Fig. 3).

Interestingly, the authors investigated relatively few different functionalities as pendant arms. They did report the synthesis of macrocycles **2** and **3** possessing ester and alcohol-functionalized side-arms [11]. Alkylation of the cyclen/glyoxal-derived bis-aminal compound with ethyl bromoacetate, followed by linkage with *m*- or *p*-xylyl dibromide readily afforded the polyammonium salt as above. In lieu of transamination with hydroxylamine or hydrazine, the authors neutralized the products via sodium borohydride reduction, thus forming the corresponding cross-bridged bis-cyclen derivatives [12]. Depending on reaction conditions (e.g. solvent selection), the products were either alcohols or the unreduced esters (Scheme 3).

Archibald and Hubin have shown that glyoxal-derived mono-*N*-alkylated aza bis-macrocycles undergo reductive ring cleavage to form the side-bridged derivatives [13a]. In particular, the gly-

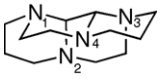

Fig. 3. A depiction of the cyclam-glyoxal condensate showing the greater steric availability of convex-pointing N1 and N3.

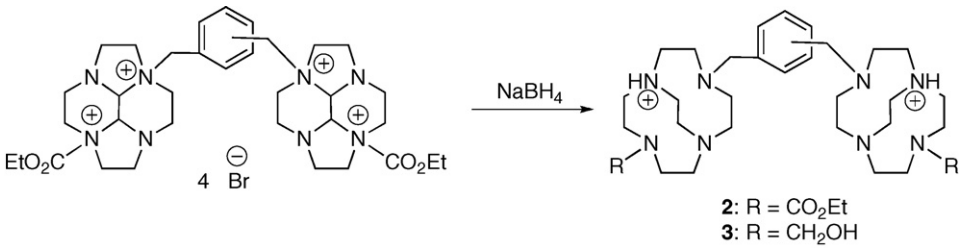

Scheme 3.

oxal derivative of cyclam was linked with *p*-xylyl dibromide, then reduced with sodium borohydride to afford **4a** (Scheme 4). Exhaustive methylation of the linked bromide salt, followed by sodium borohydride reduction gives the cross-bridged cyclam analogue **4b** (Scheme 4) [13b].

Averin, Beletskaya, and co-workers exploited the bis-aminal methodology in their synthesis of bi- and polycyclic cryptand-type compounds (Scheme 5) [14]. Treatment of the cyclen/glyoxal-derived bis-aminal with 2 equivalents of α,3-dribromotoluene in acetonitrile, followed by aminal deprotection with aqueous base resulted in the desired dialkylated macrocycle. Buchwald amination [15] using a variety of terminal diamines led to mixtures of the expected cryptands as well as tricyclic cryptands resulting from [2 + 2] cyclocondensation.

A similar strategy was employed for the preparation of xylylene bridged hexaacetate bis-macrocycles (Scheme 6) [16]. Initially, the linkage was performed on the glyoxal derivative of cyclen to afford the standard xylylene-linked bis-macrocycles **5** and **6**. Exhaustive treatment with ethyl bromoacetate afforded the hexaesters, which were readily hydrolyzed with HCl.

2.1.2. Protecting group manipulation

In addition to the bis-aminal strategy brought forth by Handel and others, a variety of amine alkylation strategies have been reported for the construction of the N–N linkage of various azamacrocycles. A strategy of particular importance has been the simple linkage of tri-functionalized/tri-protected cyclen or cyclam derivatives. These methods can provide the means for an initial introduction of desired pendant arms. Additionally, differentially protected azamacrocycles allow for the possibility of selective deprotection/refunctionalization methods for the selective formation more complex structures than are commonly available via other techniques. The obvious disadvantage of any of these techniques, however, involves the initial selective functionalization of some reactive nitrogens while leaving one or more of the nitrogens free.

The tri-functionalized tetraazamacrocycle strategy has been extensively employed by Gunnlaugsson and co-workers in their syntheses of macrocyclic cyclen ligands. They initially reported the synthesis of tri-*N*-substituted cyclen derivative **7** in greater than 50% yield by direct alkylation of cyclen with three equivalents of the requisite α-chloroamide [17]. When performed at elevated temperature and for extended periods of time in acetonitrile, the formation of mono-, di-, and tetrasubstituted derivatives was minimized. They found that treatment of **7** with *p*-xylyl dichloride in the presence of $CsCO_3$ in methanol under Finkelstein conditions resulted in the formation of the expected bis-macrocycle **8**, albeit in a poor 10% yield [18]. An explanation for the poor yield was not presented, although under the reaction conditions a competing etherification might seem plausible (Scheme 7).

The same group also reported attempts to alkylate cyclen derivatives of the form **7** with **9** [19]. The reaction, however, was retarded by the poor solubility of **9** in the organic solvents explored and a maximum 16% yield of **10** was obtained. The poor yield and tedious workup required were overcome by performing the initial coupling reaction of **9** with a molybdenum carbonyl protected variant of cyclen [20]. This strategy allowed for the selective functionalization of a single nitrogen atom of the macrocycle. Deprotection was readily accomplished by treatment with dilute acid. Finally, amide pendant arms were introduced by treatment with the requisite α-chloroamides (Scheme 8).

Faulkner arrived at **6** by utilizing a tri-functionalized cyclen derivative [21]. Starting with the known tri-ester **11**, standard linkage with *p*-xylyl dibromide readily produced **12**. The use of the *t*-butyl esters allowed for ready cleavage by simple treatment with TFA (Scheme 9).

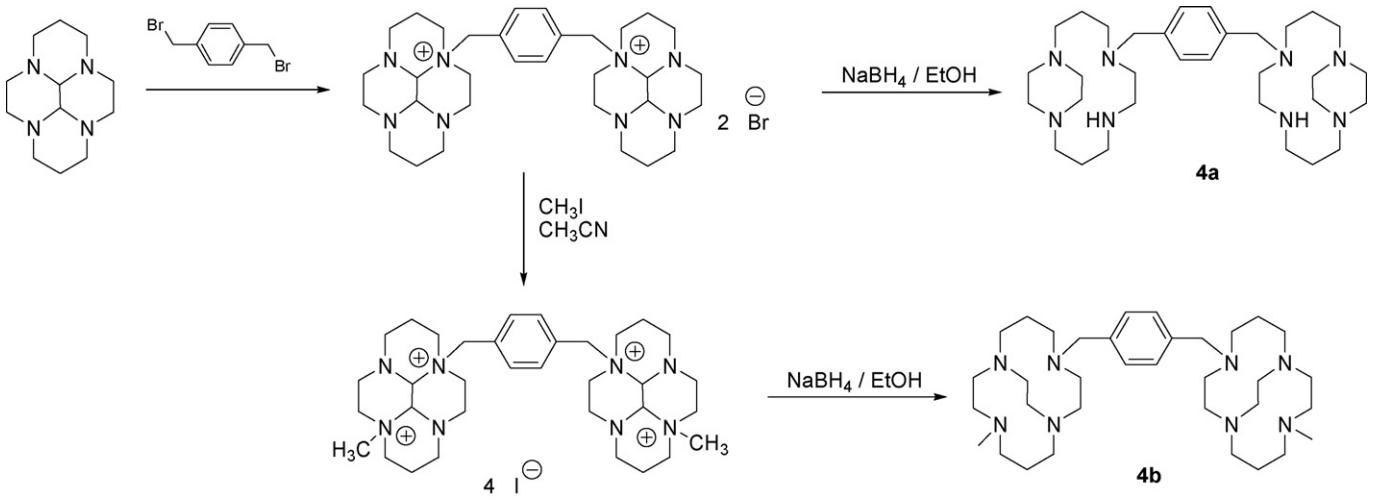

Scheme 4.

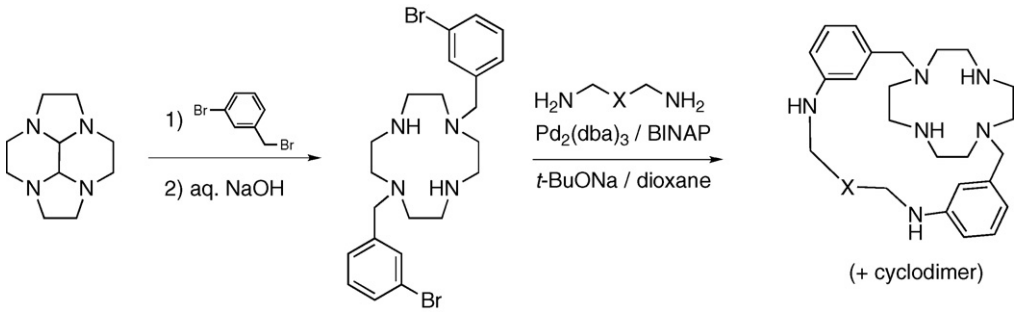

Scheme 5.

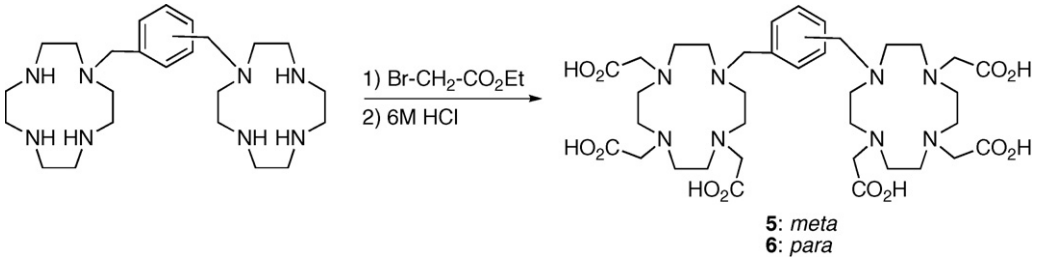

Scheme 6.

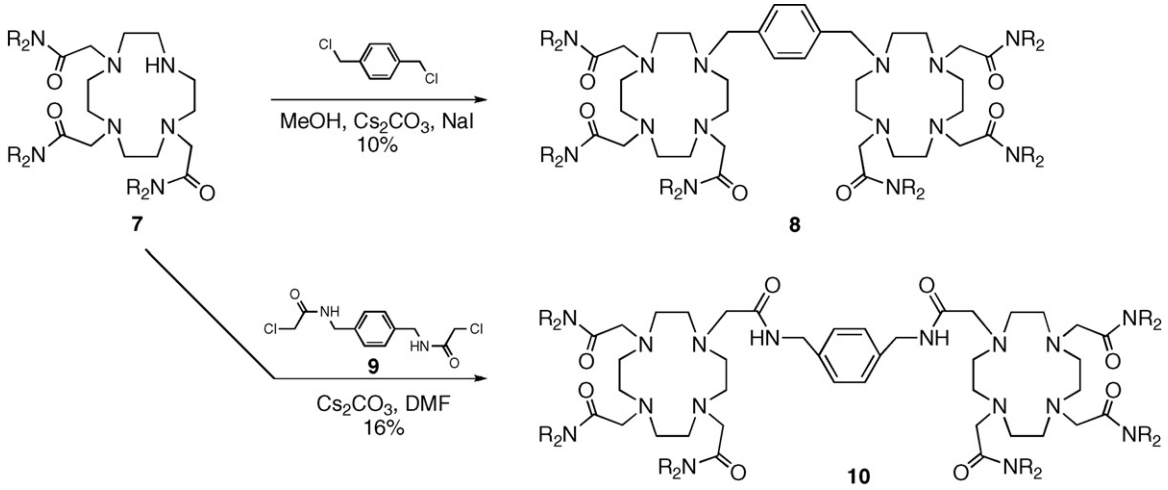

Scheme 7.

In addition, he prepared a similar ligand **13** with a phenolic linker that allowed for differentiated metal binding [22].

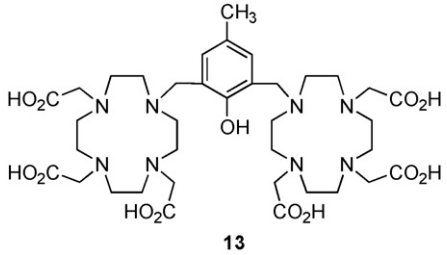

13

Wang and co-workers also reported the synthesis of a bis-cyclen scaffold functionalized with six carboxylic acid moieties (Scheme 10, **14**), albeit with a diamine linker as opposed to the more common aromatic spacer [23]. The preparation involved the coupling of the dimethyl ester of ethylenediaminediacetic acid with the tri-functionalized cyclen system. This procedure possesses the advantage of bypassing the ester hydrolysis step required in the aforementioned systems. Remarkably, the reaction was found to proceed in 88% yield, even in the presence of the amino groups of the β-amino ester starting material.

Mochizuki and Numata used *N*-benzyl protecting groups in their synthesis of an unsymmetrical bis-macrocycle ligand based on the 1,4,7-triazacyclononane (tacn) scaffold [24]. The known dibenzylated tetraazamacrocycle **15** [25] was treated with epichlorohydrin, followed by tacn to afford diprotected bis-macrocycle. This intermediate was easily debenzylated under catalytic hydrogenation conditions to afford **16**. The use of epichlorohydrin (instead of the more common dihalide moiety) in this synthesis is notable in that it allowed for a linker functionalized with an alcohol moiety capable of coordinating a metal center. Furthermore, the use of such an electrophile allows for differentiated reactivity and the ability to easily control selectivity of nucleophilic addition (Scheme 11).

Desreux and co-workers also employed an epoxide ring opening reaction in the synthesis of an alcohol-functionalized ligand based on the cyclen and 1,10-phenanthroline scaffolds [26]. The authors reported two different routes towards **17**, both originating

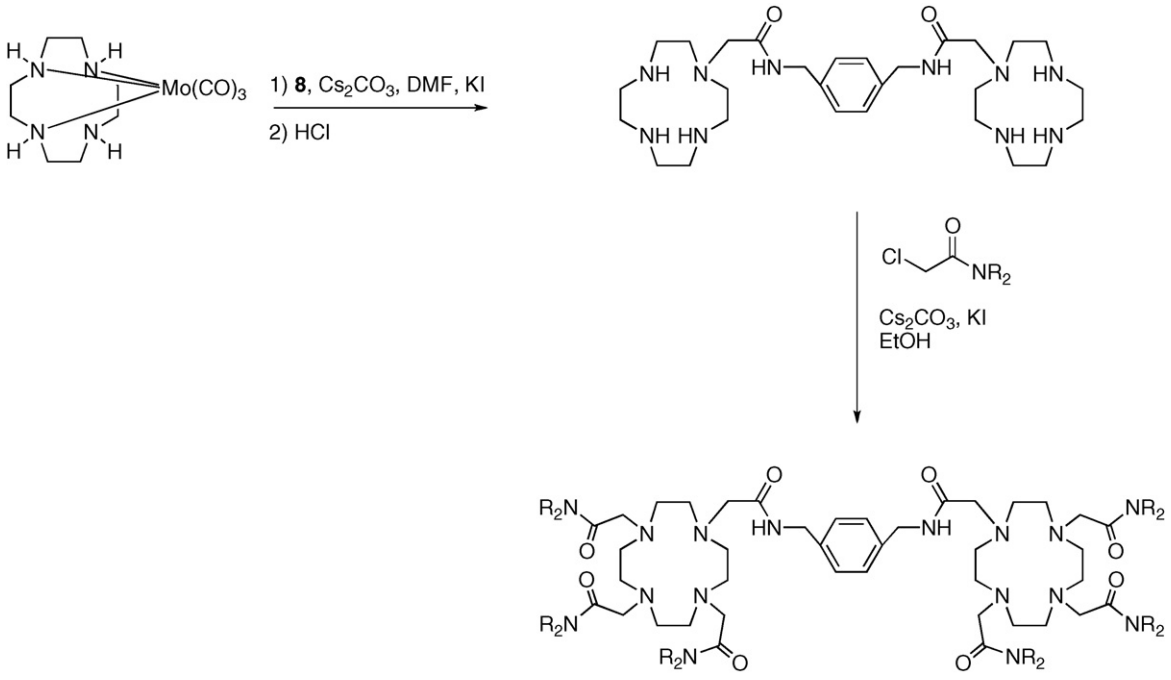

Scheme 8.

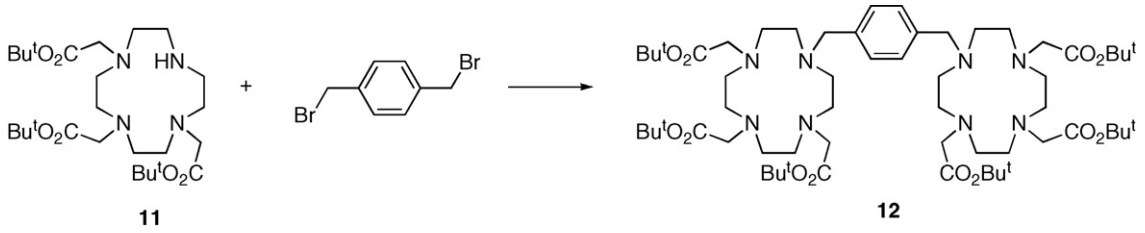

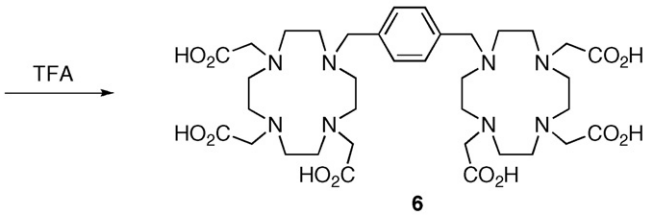

Scheme 9.

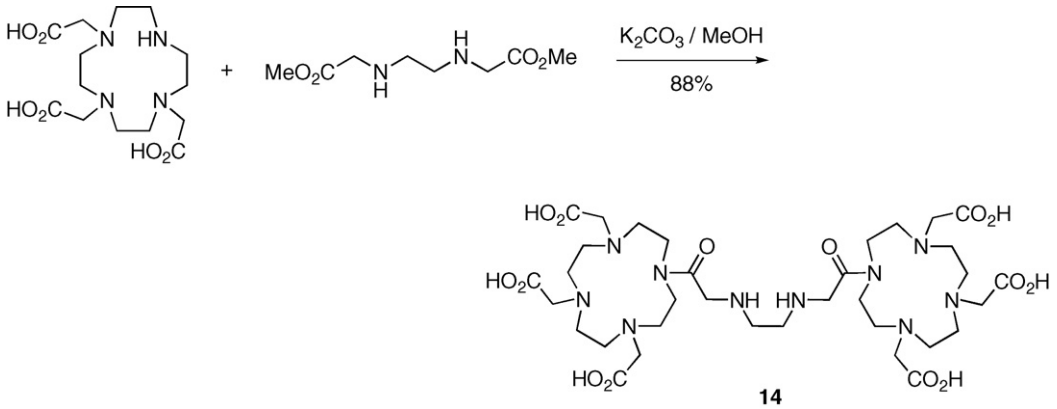

Scheme 10.

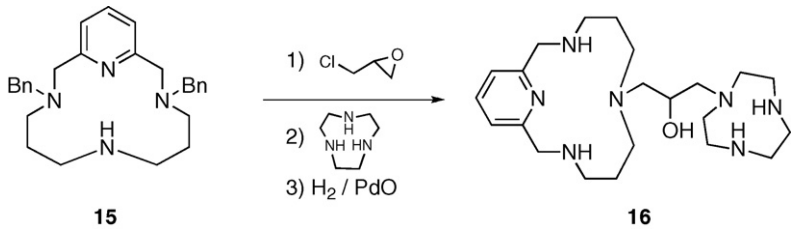

Scheme 11.

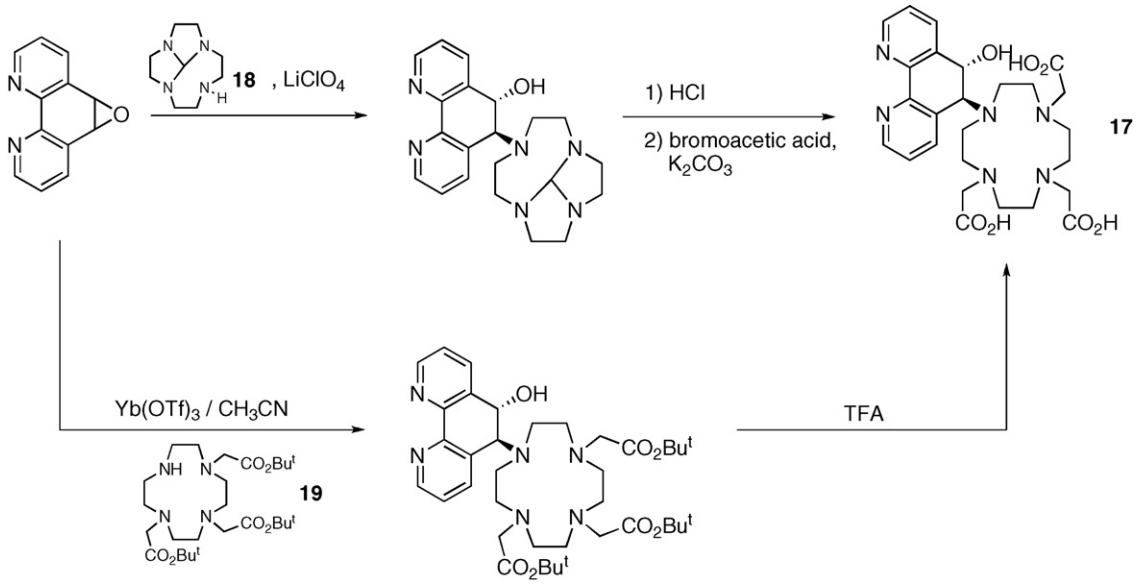

Scheme 12.

with the epoxide formed from treatment of 1,10-phenanthroline with bleach. The first route commenced with an epoxide ring opening with tetraazamacrocycle **18** followed by alkylation with bromoacetic acid to afford **17**. In the second route, tri-*t*-butyl ester **19** was utilized as the nucleophile for a ring opening of the epoxide. The reaction was found to be quite sensitive to reaction conditions, with any unreacted **19** resulting in a quite tedious chromatographic separation of esters. Best results were obtained using a $Yb(OTf)_3$ catalyst and acetonitrile as the solvent. Subsequent treatment with TFA liberated free acid **17** (Scheme 12).

Peters and co-workers prepared a bis-cyclam ligand with an alcohol-functionalized linker by treatment of tri-Boc-protected cyclam with 1,3-dibromo-2-propanol [27]. This approach mirrored previous syntheses reported by the groups of Sessler [28] and Morrow [29] in their respective syntheses of 1,3-bis(tacn)-2-propanol and represents a satisfactory method for the preparation of symmetrical bis-macrocycles. Exhaustive Boc-deprotection using HCl, followed by neutralization generated the target molecule **20** (Scheme 13).

Tri(*N*-Boc)cyclam **21** has been found to be a suitable precursor for the synthesis of unsymmetrical heteroditopic ligands [30]. Protection of cyclam with substoichiometric quantities

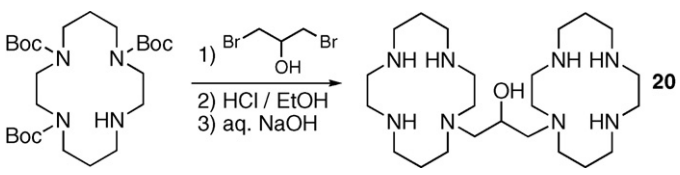

Scheme 13.

of di-*t*-butyldicarbonate (Boc_2O) led to a chromatographically separable mixture of Boc-protected derivatives [31]. The tri-protected derivative was carried forward in a reaction with 4-(chloromethyl)benzoyl chloride **22** to afford the expected amide. The use of this acid halide allowed for a selective stepwise coupling of heterocycles and minimization of homocoupling due to the greater propensity for *N*-acylation when in competition with *N*-alkylation. Coupling of the second heterocycle **23** under Finkelstein conditions led to the bis-macrocycle. Boc-deprotection using TFA, followed by borane-mediated carbonyl reduction led to the fully deprotected N–N linked macrocycle **24**. This general strategy was found to be useful for the synthesis of a number of bis-macrocycles of various ring types (Scheme 14).

The same group employed a similar strategy for the synthesis of a similar series of heterotritopic and cofacial ligands of the type **25** and **26** [32]. These syntheses required quantities of orthogonally di-*N*-protected cyclam. Such a requirement typically poses a challenge with regard to selectivity of protection, as well as isolation of the desired protected macrocycle. The researchers avoided the problems associated with low selectivity of protection by employing as starting material the orthogonally dibenzylated cyclam, a selective synthesis of which had previously been reported [33]. Boc-protection with the requisite anhydride was followed by debenzylation via catalytic hydrogenation to afford the di-Boc-protected species in quantitative yield over two steps. Treatment of this heterocycle with a substoichiometric quantity of TrocCl afforded a mixture of the mono- and di-Troc protected, with the desired mono-protected compound being formed in a 46% yield. Substoichiometric quantities (0.8 equiv.) of TrocCl were required for maximum yield; the use of greater quantities led to lower yields due to competitive diacylation (Scheme 15).

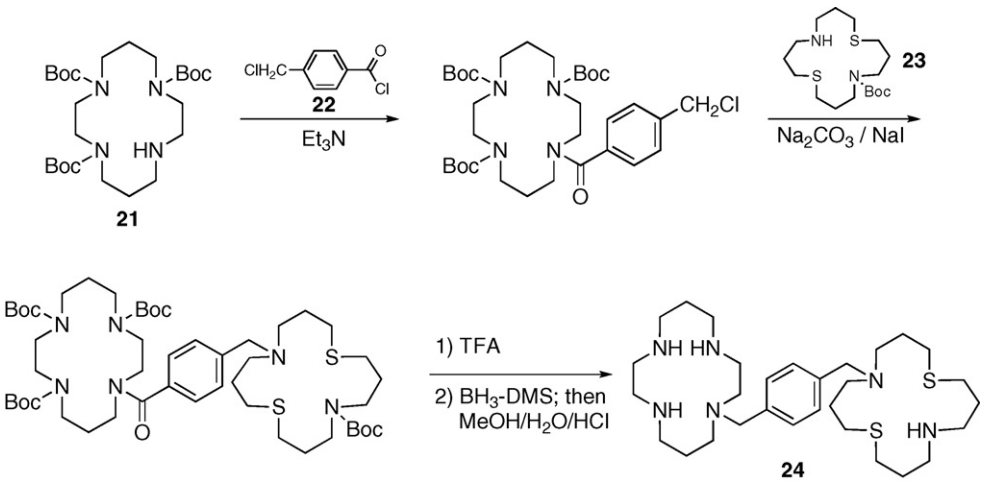

Scheme 14.

For the synthesis of heterotritopic ligand **25**, the amidation was carried out as before with 4-(chloromethyl)benzoyl chloride, followed by treatment with the Boc-protected N_2S_2-macrocycle **23**. Troc-deprotection was readily performed by treatment with Zn/HOAc and the resulting product was subsequently again amidated with 4-(chloromethyl)benzoyl chloride. Treatment of this with aza-crown ether **27** afforded **25** after standard Boc-deprotection and carbonyl reduction (Scheme 16).

Synthesis of cofacial ligand **26** required the use of di-Troc protected compound **28**. Troc-deprotection of **28** was followed by cyclization in the presence of terephthaloyl dichloride. The cyclization protocol required the use of highly dilute conditions in order to minimize polymerization. Boc-deprotection and carbonyl reduction as before resulted in the formation of **26** (Scheme 17).

Lindoy, Smith, and co-workers also utilized 4-(chloromethyl) benzoyl chloride to affect the bis linkage of **29** with two equivalents of tri(*N*-Boc)cyclam in their preparation of three-ring macrocycles, such as **30** [34]. Amidation of **29** with the acid chloride occurred selectively on the amine nitrogens, thus setting the stage for displacement with tri(*N*-Boc)cyclam (Scheme 18).

Beer and Gao exploited the latent functionality of the 3-nitrobenzyl protecting group in the synthesis of N–N linked macrocyclic dendrimers [35]. This work represents the first example of a dendrimer containing the tacn subunit. The core was prepared by treatment of 1,4,7-triazacyclononanone with 3-nitrobenzyl chloride, followed by reduction of the nitro groups with H_2/Raney Ni. The resulting triamino compound was subjected to standard amide coupling to afford the first generation dendrimer **31** in 90% yield (Scheme 19). A subsequent Raney Ni reduction/amide coupling sequence was utilized to form the second generation dendrimer in 60% yield.

2.1.3. Template cyclization

Whereas the previous syntheses have primarily focused on the construction of bis-macrocycles by the coupling of two or more macrocycles with an appropriate tether, a powerful alternative involves the coupling of acyclic precursors for the construction of the macrocyclic ring systems. For N–N linked macrocycles, this has very commonly involved an aldehyde/diamine condensation to form an imine. In such circumstances, assembly of the macrocycle is quite often controlled by the presence of an N-ligated metal (e.g. Cu or Ni) used to bring the ends of the acyclic molecules into the proximity required for cyclization. These methods typically have the advantage of being direct and brief; however, they commonly suffer from poor yields and the inability to selectively produce unsymmetrical ligands.

An illustrative example of this type of reaction was reported by Kim and co-workers [36]. They reported the treatment of **32** with $CuCl_2$, followed by reaction with ethylene diamine and formaldehyde in the presence of triethylamine to accomplish the synthesis of **33** in 19% yield (Scheme 20). Although the yield was unremarkable, the brevity of the synthesis of the ligand/macrocycle complex is noteworthy.

Mochizuki reported a synthesis of **35**–**Cu** complex by reacting hexaamine **34** with 2,6-diformylpyridine in the presence of $Cu(NO_3)_2$ [37]. The initially formed imine was then reduced with $NaBH_4$ to give **35** as the Cu complex. The authors found that the metal-free ligand **35** could be obtained by reaction of this complex with NaCN (Scheme 21).

Salavati-Niasari and Amiri reported a one-pot multi-component construction of a bis-macrocycle using Ni^{2+} coordination as a key ring-formation strategy [38]. An appropriate aromatic diamine was treated with formaldehyde, followed by 1,3-diaminopropane, Ni^{2+} salt, and 2,4-pentanedione to afford the N–N linked cycle **36**–**Ni** (Scheme 22, illustrated with diamine = *p*-phenylenediamine).

2.2. C–C linking

Although N–N linkage of bis-azamacrocycles is a popular technique due to the nucleophilicity of the nitrogens involved, carbon–carbon linkages are also not uncommon. Inspired in no small part by the seminal work of Busch and co-workers [39], a number of reports of macrocyclic bis(cyclidene) ligands and their corresponding transition metal complexes have appeared in

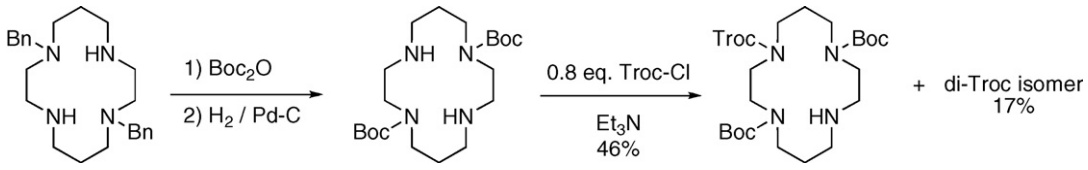

Scheme 15.

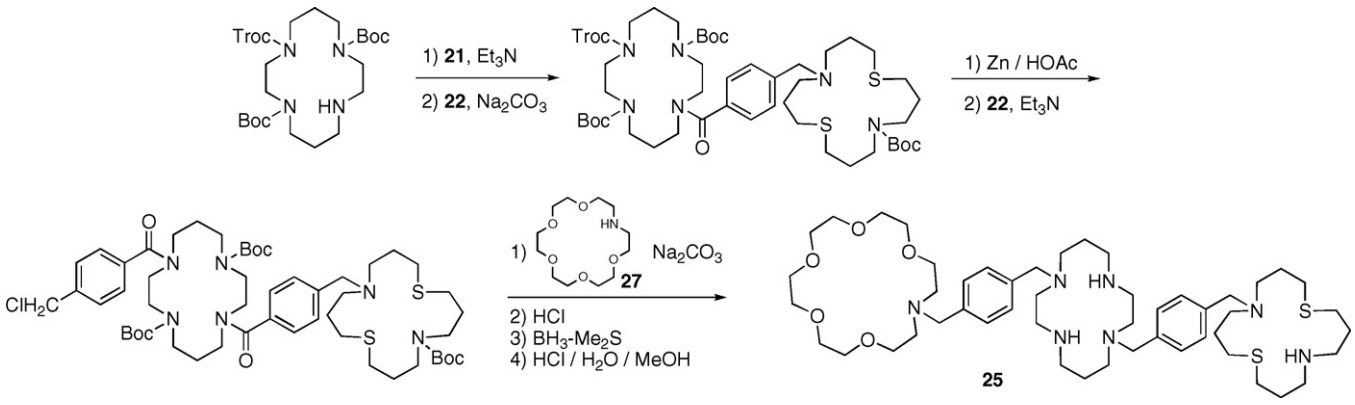

Scheme 16.

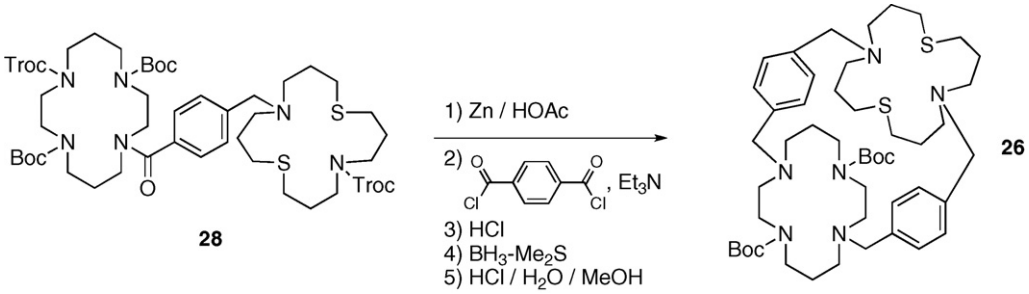

Scheme 17.

recent years. A common theme found in a number of these syntheses involves the reaction of bis enol ethers with diamines to afford C–C linked macrocycles tethered by diaminoalkyl linkers of various chain lengths. Such methodology typically allows for the initial complexation of various metals into the macrocycles and, as a result, either homo- or heterodinuclear complexes are readily attainable.

Korybut-Daszkiewicz and co-workers reported several homodinuclear cyclidene complexes of Cu and Ni [40]. Enamine/aldehyde complex **37**–**M** (M = Cu or Ni) was readily *O*-methylated by treatment with methyl trifluoromethanesulfonate to afford enol ether **38**–**M**. Treatment with terminal diamines accomplished cyclization to afford the metal-complexed macrocycles **39**–**M** (Scheme 23).

It is noteworthy that when the reaction was carried out under certain conditions, specifically when employing 1,7-diaminoheptane and excess dibenzo-24-crown-8 under highly dilute conditions, a novel catenation process resulted, affording **40**–**M**. Unlike "normal" catenanes formed by direct coordination of the metals, the authors reported that π–π interactions between the aromatic and the cyclidine rings were the primary attractions controlling cyclization (Scheme 24).

Another example of the heterodinuclear methodology was recently reported by the same group [41]. Copper complex **38**–$\mathbf{Cu^{2+}}$ was treated with various terminal diamines to affect an exchange of the alkoxide groups of the enol ethers for the amines. Treatment of this with nickel complex **38**–$\mathbf{Ni^{2+}}$ afforded the heterodinuclear Cu/Ni complex **41**–$\mathbf{Cu^{2+}Ni^{2+}}$. The final coupling step proceeded in a somewhat low yield (15%). This is in part attributable to the competitive formation of both the Cu^{2+}/Cu^{2+} (15%) and the Ni^{2+}/Ni^{2+} (10%) homodinuclear complexes under the reaction conditions. The authors later found that the same type of synthesis was possible using *N*,*N*-dimethylated diamines, thus producing tetra-*N*-methylated bis-macrocycles [42] (Scheme 25).

By a quite different strategy, Wang and Lönnberg created a small library of di- and tri(azacrown) complexes based on the 1,5,9-triazacyclododecane scaffold [43]. The synthesis commenced with the formation of the benzaldehyde/glycerol acetal. Benzylation of the remaining free hydroxyl group, followed by acetal cleavage and tosylation under standard conditions afforded **42**. Displacement with 1,5,7-triazabicyclo[4.4.0]dec-5-ene (TBD) followed by $NaBH_4$ reduction afforded the corresponding orthoamide. This was fully deprotected to liberate the free alcohol and amines by reac-

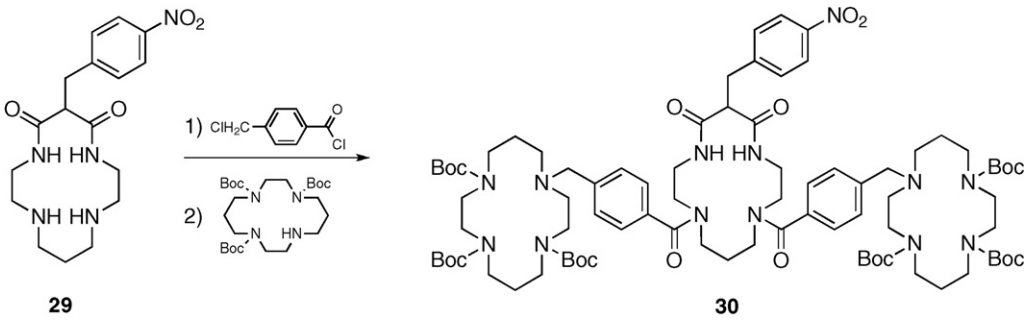

Scheme 18.

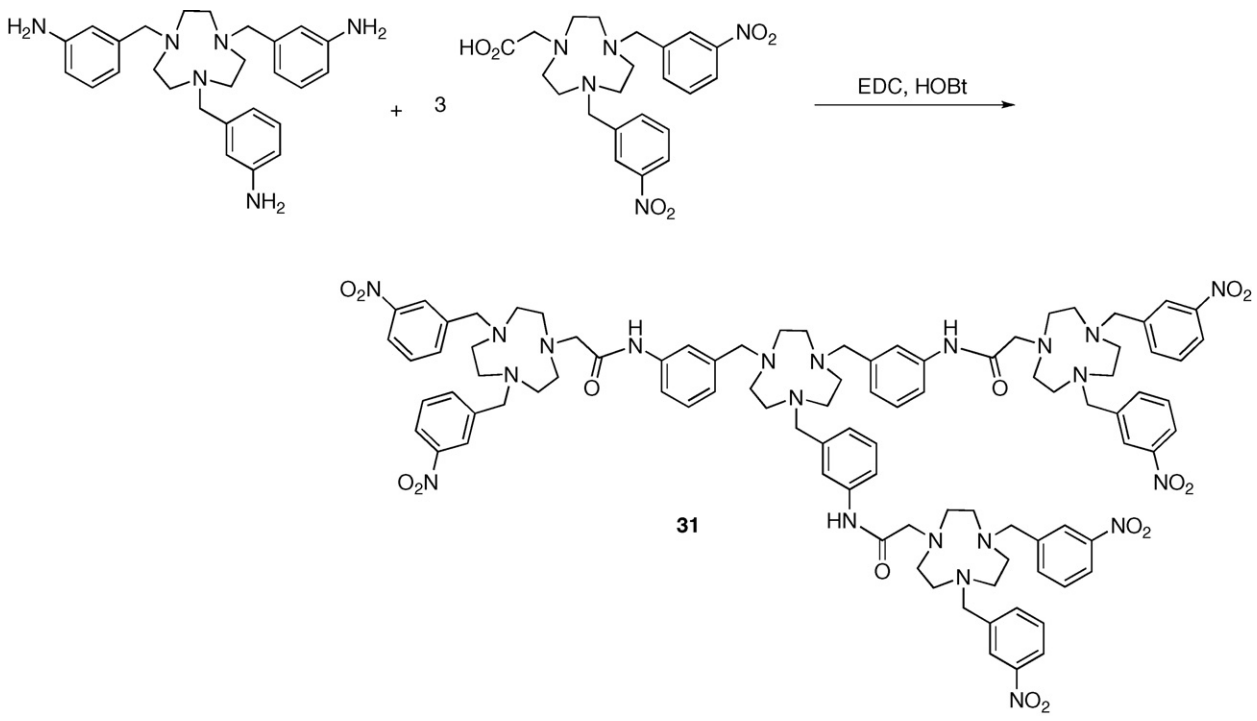

Scheme 19.

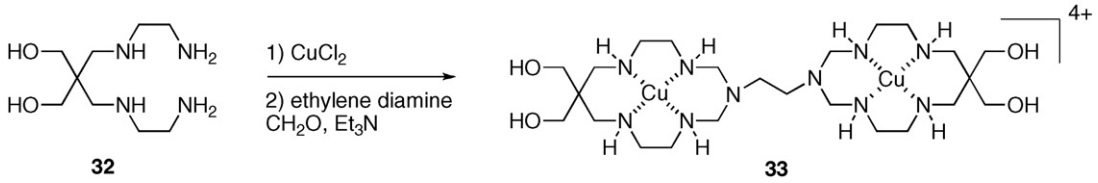

Scheme 20.

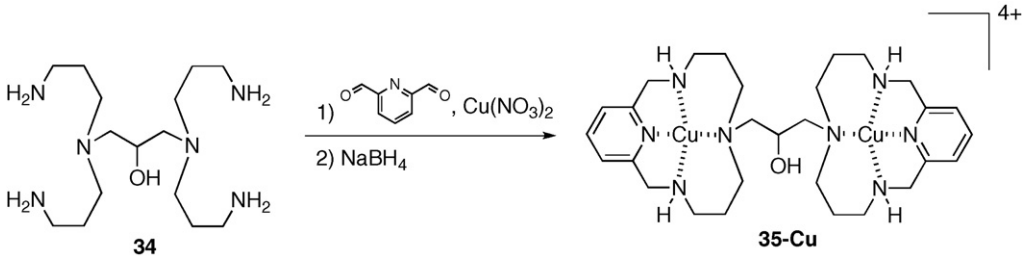

Scheme 21.

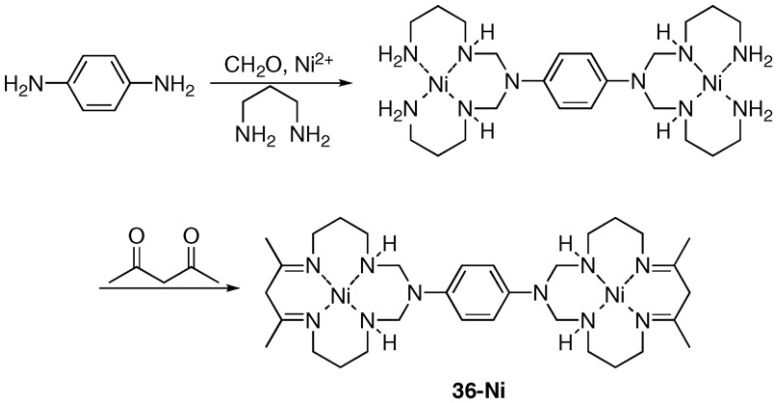

Scheme 22.

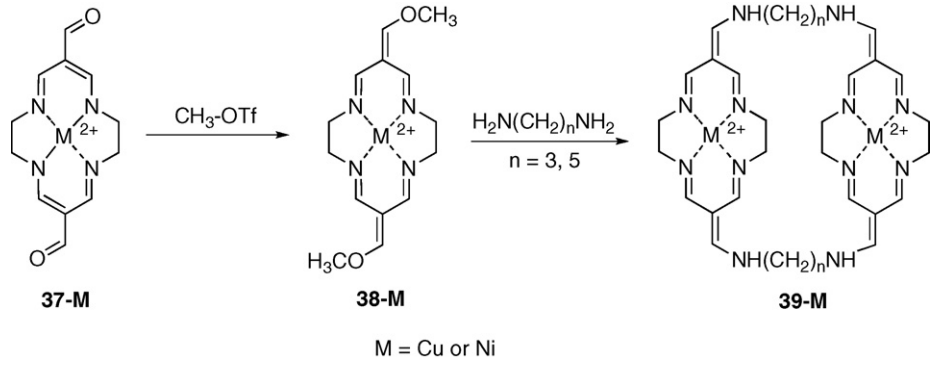

Scheme 23.

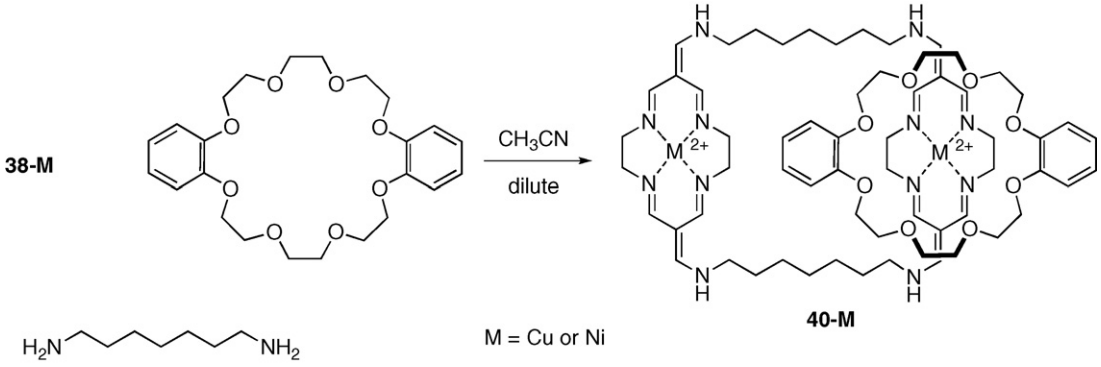

Scheme 24.

tion with aqueous HCl and the free amines were again protected as their Boc derivatives to produce **43** (Scheme 26).

Coupling of the free alcohol **43** with a variety of benzylic di- or trihalides resulted in the formation of the corresponding di- and tri(azacrown) compounds which could be exhaustively deprotected again by treatment with aqueous HCl (Scheme 27, shown with benzylic dihalide = 1,4-di(bromomethyl)benzene).

3. Applications of linked azamacrocycle ligands

3.1. CXCR4 antagonists

Clearly, the most famous application of linked azamacrocycles to date has been their use as medicinal compounds, utilizing their ability to bind to the CXCR4 chemokine receptor [44]. Interestingly,

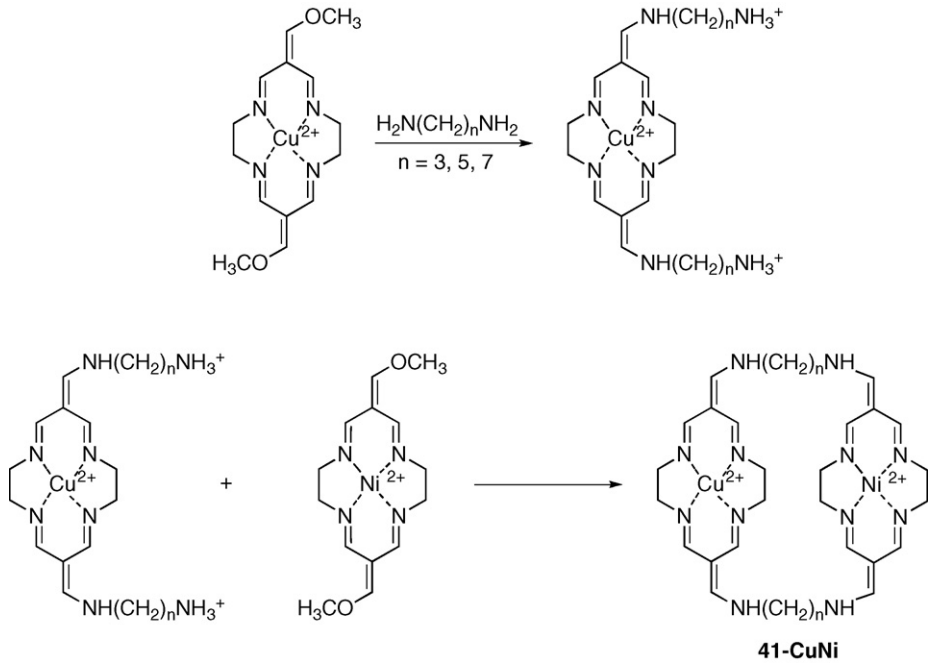

Scheme 25.

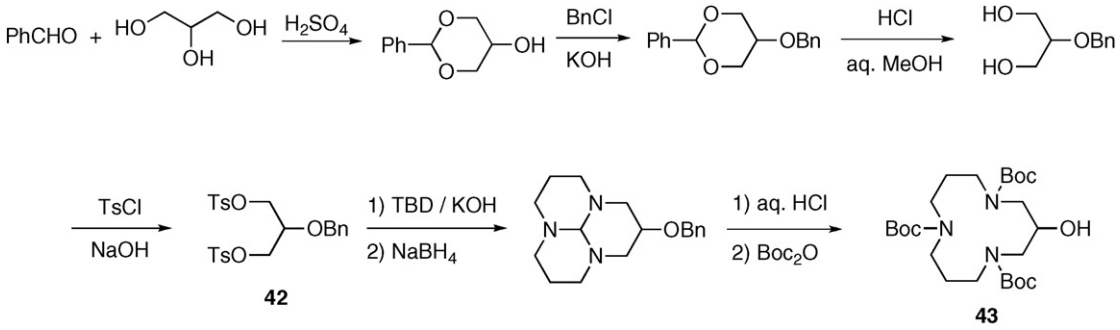

Scheme 26.

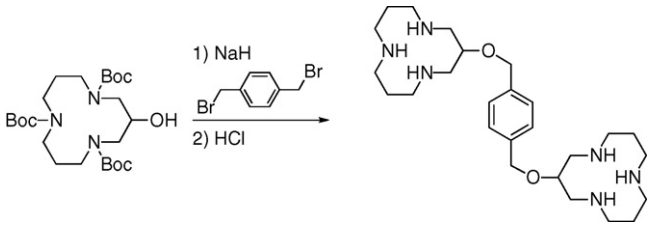

Scheme 27.

the discovery of this biological activity intersects with one of the earliest linked azamacrocycles. Virologist De Clercq and co-workers discovered that an impurity in a commercial sample of cyclam was responsible for that sample's anti-HIV properties [45,44b]. The impurity turned out to be a C2–C2′ linked bicyclam (**44**) initially identified and published by Barefield in 1981 [46]. Subsequent work determined that an aromatic linking group greatly enhanced the activity of the compounds, and the previously synthesized compound now well known as AMD3100 (**45**) was launched [47]. This compound has recently been approved as a commercial drug [48] (Plerixafor; Mozobil), although for stem cell mobilization rather than as an antiviral.

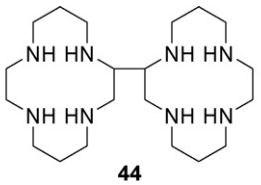

44

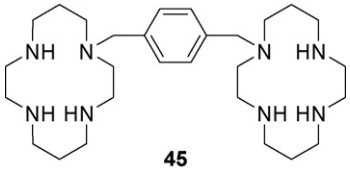

45

Receptor mutagenesis studies where Asp residues were mutated to Asn followed by AMD3100 binding experiments determined that Asp171 and Asp262 of CXCR4 were the probable binding sites for bicyclams [49]. It is likely that each cyclam ring is protonated at physiological pH and can hydrogen bond with the Asp carboxylate groups. In addition to the potential for hydrogen bonding to CXCR4, complexation of Zn^{2+} (~20 μM in blood plasma) to AMD3100 is likely *in vivo* [50]. If this occurs, coordination of Zn^{2+} to the aspartate carboxylates may actually provide the interaction with CXCR4 *in vivo*. In this case, AMD3100 would be acting as a prodrug, with the metal complex the active drug.

A large catalog of AMD3100 analogues has been prepared and evaluated for their HIV activity [51]. The systematic studies included changing the macrocycle ring size (cyclam, cyclen, homocyclen, 15[ane]N4, 16[ane]N4, *iso*-cyclam) and the linker (*m*-xylyl, *p*-xylyl, all of the dimethylene pyridyl and pyrazyl linkers, and various monosubstituted *meta* and *para* xylenes). AMD3100 (**45**) has continued to be the lead compound for CXCR4 interaction [48]. Transition metal complexes of AMD3100 and of numerous analogues as improved AMD3100 analogues will be discussed in Section 4.4.

CXCR4 antagonists based on linked azamacrocycles will likely continue to garner interest by medicinal and coordination chemists. CXCR4 chemokine receptors are found on the surface of immune, and other, cells, and together with the specific natural ligand, stromal cell-derived factor-1α (SDF-1α, also known as CXCL12), play a role in a number of disease states other than HIV and stem cell transplantation. For example, the CXCR4–CXCL12 system is involved in a number of inflammatory diseases, and the development of rheumatoid arthritis [52]. CXCR4 expression has also been reported in at least 23 different epithelial, mesenchymal and hematopoietic cancers [53]. CXCL12 stimulation of tumor growth, angiogenesis, and metastasis of breast cancer cells has been described [54]. Target organs for breast metastases such as liver, lung, and bone have high levels of CXCL12, triggering the specific migration of breast tumor cells that express the CXCR4 receptor [55]. Undoubtedly, further work utilizing linked tetraazamacrocycle drug candidates to combat these CXCR4-related diseases is warranted.

3.2. Anion and small molecule receptors

An early example of anion binding to linked azamacrocycles was published in 1990 [56]. Protonated pentaaza- and hexaazamacrocyles had demonstrated an ability to bind anions [57]. Kimura and co-workers posited that linking two such molecules might improve anion binding, and thus produced polyether and propylene linked pentaazamacrocycles **46**–**47**. These ligands were evaluated titrametrically and polaragraphically for anion binding and were found to make stable 1:1 complexes with citrate^{3-}, AMP^{2-}, ATP^{4-}, HPO_4^{2-}, $[Fe(CN)_6]^{4-}$ and $[Fe(CN)_6]^{3-}$. In each case, two linked azamacrocycles always resulted in stronger anion binding than for a single azamacrocycle. This result seems logical, as it is typically easier to hold onto a macroscopic object with two hands rather than one. Chemically speaking, something akin to the chelate effect [58] is likely at work.

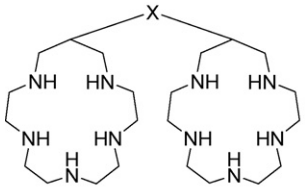

46a X = -$CH_2CH_2CH_2$-

46b X = -$CH_2CH_2OCH_2CH_2OCH_2CH_2$-

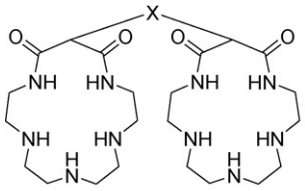

47 X = -$CH_2CH_2CH_2$-

More recently, Handel and co-workers have investigated the binding of various phosphate anions to polyprotonated linked tetraazamacrocycles [59]. Aromatic-linked cyclens **48**–**51** were studied initially [59a] by potentiometric methods and NMR spectroscopy for binding to orthophosphate, PO_4^{3-}, pyrophosphate, $P_2O_7^{4-}$, and triphosphate, $P_3O_{10}^{5-}$. Conclusions from the work included: (1) The strength of the ternary (anion, ligand, H) complexes generally increases $PO_4^{3-} < P_2O_7^{4-} < P_3O_{10}^{5-}$, which was attributed to charge–charge interactions. (2) **50**, with its pyridine linker able to contribute to the anion binding below pH 2, was the most efficient phosphate anion binder. Interestingly, at high pH 9–12, repulsion from the pyridine lone pair causes the complete release of triphosphate, making **50** a potentially useful analytical reagent.

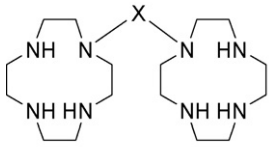

48 X = o-xylyl
49 X = m-xylyl
50 X = 2,6-dimethylpyridine
51 X = p-xylyl

Linking the same cyclen azamacrocycles a second time to produce macrotricyclic ligands (**52**–**56**) was achieved [59a] and their phosphate anion binding ability examined in a similar fashion [59b,59c]. In a result that is reminiscent of the relationship of the macrocycle effect [60] compared to the chelate effect [58], the twice-linked systems exhibited higher phosphate binding constants and selectivity compared to the once-linked analogues, which was attributed to the more rigid cavity of the macrotricyclic ligands [59b].

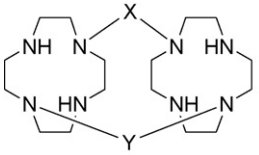

52 X = Y = o-xylyl
53 X = Y = m-xylyl
54 X = Y = 2,6-dimethylpyridine
55 X = Y = p-xylyl
56 X = m-xylyl
Y = 2,6-dimethylpyridine

Size effects were more evident in the twice-linked systems as well, especially at acidic pH's, where an increase in cavity size clearly resulted in an increase in triphosphate binding [59b]. Surprisingly, **54**, containing two pyridyl linkers that clearly increased binding efficiency compared to the xylyl linkers in the once-linked systems, is actually less efficient at triphosphate binding than **56**, with one pyridyl and one *m*-xylyl linker [59c]. A proposed explanation is that protonation of both pyridine nitrogens does not occur under the studied pH range. If one pyridine is protonated, but the other is not, the increased binding offered by the protonated pyridine is defeated by the lone pair repulsion (as observed at high pH for **50**) of the other.

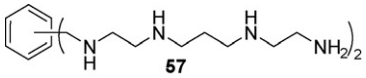

57

Handel et al. turned to an examination of triphosphate binding of linked cyclam **45** in comparison to similarly *p*-xylyl linked linear tetraamines (**57**) [59d]. Over the entire pH range studied, the linear system was a more efficient binder of triphosphate than **45**. The key factor in this result was identified as the ability of the linear system to more easily form polyprotonated species than linked azamacrocycle **45**. In addition, the flexibility of **57** allows it to more optimally fit around the triphosphate anion. The advantages macrocycles hold over linear polydentate chelates are manifold when it comes to metal ion complexation [5], but this study shows that these advantages may not be as evident when coordinating multi-atom anions such as triphosphate.

In 2008, this study was extended to AMP, ADP, and ATP complexation to **49** and **50** [61]. 1:1 complexes between all of these nucleotides and the two linked azamacrocycles were formed. As was seen in the previous phosphate anion binding studies, **50** proved to be the most efficient host molecule over the entire pH = 2–12 range. Again, the pyridine linker provides an additional point of interaction with the guest that is beneficial in terms of binding ability. A general trend observed was that binding increased as protonation of the linked azamacrocycle increased. AMP was the best guest for **49**, while ATP was particularly strongly bound to **50**, until around pH = 9. NMR studies also indicated that π–π stacking between the aromatic linker and the adenine group in ATP is likely playing a role in stabilizing the complexes. This effect appears to be pH dependent for **50**, coinciding with the pyridine linker protonation (around pH 4) and its change in role from π–π interaction with adenine when unprotonated to H-bonding to the phosphate groups at low pH (**58**).

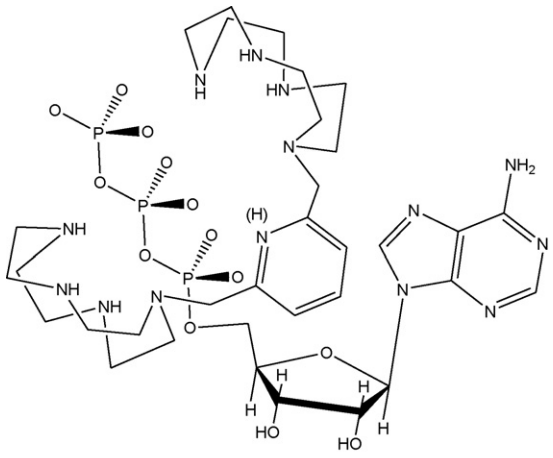

58

4. Applications of linked azamacrocycle metal complexes

4.1. Medical imaging

4.1.1. Magnetic resonance imaging

One key improvement in MRI diagnostics has been the use of "contrast agents," paramagnetic metal containing compounds administered prior to the MRI scan that enhance the resolution of the image by accelerating the nuclear relaxation of tissue water protons. Contrast agents are now used in about 30% of all MRI exams [62]. Gadolinium(III) is the preferred metal ion to use, since its seven unpaired electrons result in the largest magnetic moment for any metal ion, and thus provides the largest resolution gains. Gd^{3+} alone is quite toxic, so clinically useful contrast agents must bind the metal ion in an organic ligand that will shepherd the metal ions safely through the patient. Currently used macrocyclic contrast agents typically contain a DOTA [63] type ligand (**59**) bound to only one Gd^{3+} ion per molecule (**60**), and usually have relaxivities (a measure of effectiveness) of about 3–5 $mM^{-1}\,s^{-1}$.

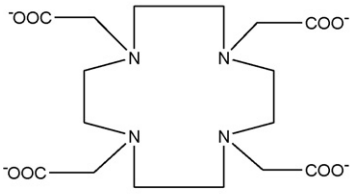

59 DOTA

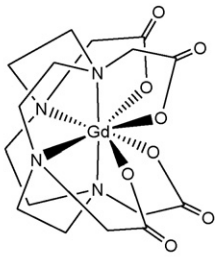

60 Gd(DOTA)-

Improving the relaxivity (R_1) of contrast agents has been a long-standing goal of inorganic chemists. The Solomon–Bloembergen–Morgan theory predicts that a relaxivity over 100 $mM^{-1}\,s^{-1}$ could be achieved by the manipulation of four key factors: the number of open coordination sites available to interact with water, electron spin relaxation rates, water exchange rates, and molecular reorientation [64]. The electron spin relaxation rate has not yet lent itself to rational optimization. However, each of the other areas has been individually improved through rational design of new ligands to bind Gd^{3+}. The factor most relevant to linked azamacrocycles that has been modified independently for optimization of relaxivity is molecular reorientation (τ_R). To optimize this factor, the usual approach has been to synthesize large molecules that slowly tumble (or change their orientation) in the aqueous matrix of the bloodstream. The relevant approach is to design ligand systems that are large themselves, perhaps containing multiple Gd^{3+} centers [65].

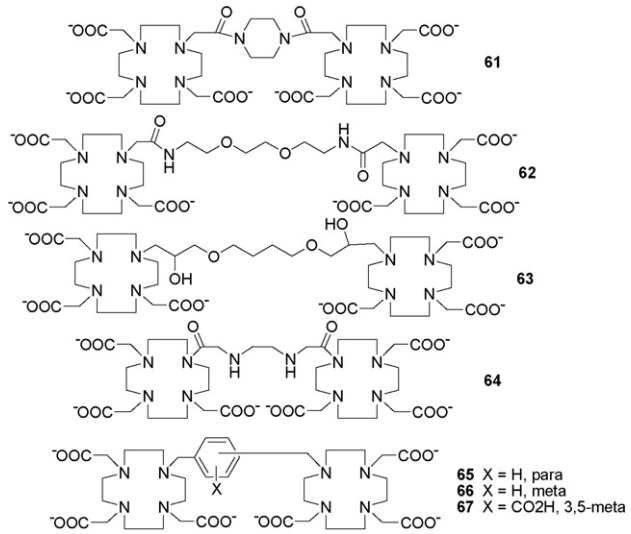

61

62

63

64

65 X = H, para
66 X = H, meta
67 X = CO2H, 3,5-meta

Linked azamacrocycles prepared for this purpose have largely contained DOTA (**59**) derivatives where one of the acetate pendant arms has been replaced with a linker (**61–67**). The Gd_2(**63**) complex [66] was found to have a 3-fold increase in τ_R compared to **60** as expected for the larger molecule, but the overall increase in relaxivity was only modest: 4.61 $mM^{-1}\,s^{-1}$ per Gd compared to 3.4 $mM^{-1}\,s^{-1}$, respectively. The less than expected enhancement of R_1 reflected an unanticipated reduction in the water exchange rate by a factor of 5 compared to **60**. Apparently, the smaller, more weakly donating hydroxo group is not as effective as another carboxylate donor in forcing water dissociation.

The novel linked azamacrocycles **61** and **62** Gd_2 complexes were included in the first integrated analysis of ^{17}O NMR, EPR, and NMRD data for a series of known Gd^{3+} mononuclear MRI contrast agents, including the three commercially used contrast agents at that time [67]. Interestingly, it was found from the EPR data that the dimeric complexes had transverse electronic relaxation rates much greater than the monomeric species and that the temperature dependence of these rates changed in the opposite direction compared to the monomers. The conclusion was that a previously undocumented additional contribution to electronic relaxation due to intramolecular dipole–dipole interactions between the Gd^{3+} ions was the cause of this unusual behavior. Unfortunately, the enhancement of the overall relaxivity due to this effect is relatively minor compared to other factors, such as the water exchange rate.

An enhancement of relaxivity due to slower tumbling as measured by τ_R was also observed for the dimeric complexes. This relaxivity enhancement was larger for the **61** complex (171 ps) than for the complex of **62** (106 ps) vs. τ_R = 77 ps for **60** [67]. The data suggests that the more flexible linker of **62** allows the linked complexes to rotate independently of each other mitigating the desired effect of linking the complexes together. The authors point out that the rigidity of the linker in effective dimeric contrast agents must be such that the entire complex rotates as a whole in order to take advantage of an enhanced τ_R.

Finally, as in Gd_2(**62**), sacrificing carboxylate ligands in order to link the azamacrocycles results in less crowding, and slower dissociative water exchange rates [$1.5 \times 10^6\,s^{-1}$ for Gd_2(**61**) and $1.4 \times 10^6\,s^{-1}$ for Gd_2(**62**) vs. $4.1 \times 10^6\,s^{-1}$ for Gd(DOTA) = **60**]. The authors recommend screening any potential polymeric MRI contrast agents by studying their dimeric analogues in order to ensure that the linker rigidity and the water exchange rates are optimized prior to synthesizing the polymeric versions. Overall, the increases in relaxivity at 40 °C due to enhanced electronic relaxation and molecular reorientation are a modest [68] [5.8 $mM^{-1}\,s^{-1}$ per Gd for Gd_2(**61**) and 4.9 $mM^{-1}\,s^{-1}$ per Gd for Gd_2(**62**)] vs. the value of 3.4 $mM^{-1}\,s^{-1}$ for Gd(DOTA) = **60**.

Linked azamacrocycle **64** was examined in its Gd^{3+} complex as an MRI contrast agent as well [23]. As expected, τ_R for this complex (105 ps) was significantly higher than for the **60** (77 ps) monomer. This value is similar to the one noted above for the **62** complex (*vide supra*). Therefore, it appears that the flexible ethylenediamine linker has the same disadvantage as the flexible polyether linker of **62**. The water exchange rate for the **64** Gd complex was found to be $1.3 \times 10^6\,s^{-1}$, which is similar to the values for the other dimers discussed and much slower than in **60**, with a similar explanation of lack of steric crowding of the bound water molecule given by the authors. The R_1 value for the **64** Gd complex, reflecting all of these factors, is 3.60 $mM^{-1}\,s^{-1}$ per Gd [23].

Ligands **65–67** [16] were synthesized to take advantage of the rigidity of the xylene core, a property confirmed in xylyl

linked non-cylic systems [62]. An additional change in these ligands is that no coordinating function has been added to the linker, leaving the ligands heptadentate, and potentially allowing for more water molecule coordination. Measurements, however, proved that each Gd complex with these ligands only had one water molecule per Gd. Interestingly, the aromatic linkers appear to promote aggregation of the neutral Gd complexes in water. The large aggregates lead to slow rotation. From NMRD studies, $\tau_R = 889$, 570, and 974 ps for the complexes of **65**–**67**, respectively. An additional advantage these complexes demonstrate is a water exchange rate much higher than the previously discussed linked azamacrocycle systems. The values presented are 7.5×10^6, 11.0×10^6, and 12.0×10^6 s^{-1} for the complexes of **65**–**67**, respectively. Relaxivities characterized [16] as "remarkably high" and "twice as high as for nonaggregated complexes of similar size" were observed for these aggregates. Unfortunately, exhaustive attempts at disaggregating the particles in order to study the individual complex properties, including their relaxivities, failed.

An MRI contrast agent taking advantage of coordination chemistry for linking multiple rings was published in 1999 with more details being recently provided [26,69]. Complex **68** links three DOTA-like macrocycles through coordination of a phenanthroline pendant arm to a central Fe ion. Compared to the monomer, formation of the Fe^{2+} complex results in a 4-fold increase in the rotational correlation time, owing to the large size of the trimer and its rigid architecture around the Fe^{2+}. The resulting effect on the relaxivity is an increase of 90% compared to the monomer: 12.2 mM^{-1} s^{-1} for **68**.

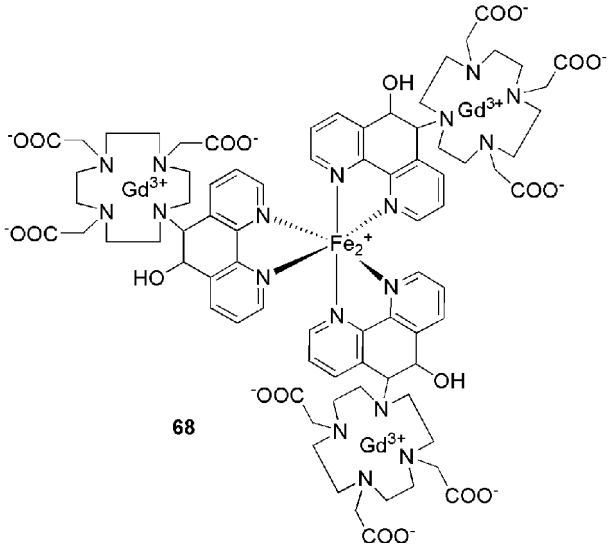

68

A final MRI contrast agent utilizing linked azamacrocycles was aimed at producing a calcium-sensitive probe [70]. This "smart" contrast agent uses a physiological trigger, Ca^{2+} concentration, to expose the Gd^{3+} to bulk water, while it is shielded from bulk water in the "silent" state. Ca^{2+} plays an important role in the nervous system, with fluctuations in concentration associated with normal and abnormal brain activity [71]. The Gd complexes of **69**–**71** represents an effort to translate the Ca^{2+} concentrations into changes in MRI contrast.

At low Ca^{2+} concentrations, some of the linker donor atoms would be bound to Gd, partially shielding Gd from interacting with water. Ca^{2+} binding would occupy the linker donor atoms, thus freeing Gd for more water interaction, and higher relaxivity.

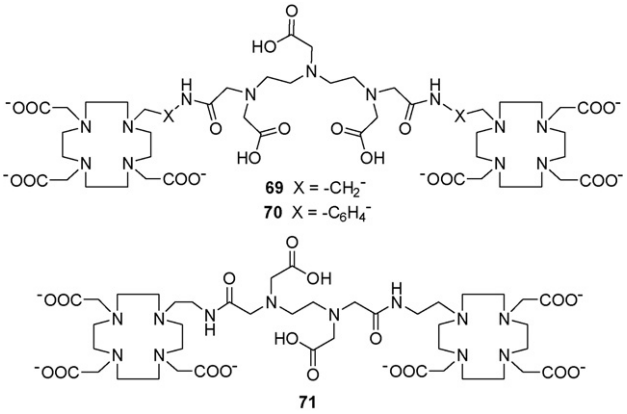

The proton relaxivities of the Gd complexes with these ligands were studied at various Ca^{2+} ion concentrations. The relaxivities in the absence of Ca^{2+} were 6.22 mM^{-1} s^{-1} with **69**, 8.19 mM^{-1} s^{-1} with **70**, and 6.05 mM^{-1} s^{-1} for **71**. While the complexes of **69** and **71** were sensitive to Ca^{2+} concentration, with the relaxivity increasing 15% and 32%, respectively, the change for the **70** complex only changed 6%. This result was attributed to the longer, more rigid separation of the Gd ions from the Ca^{2+} binding central group in **70**. Such rigidity is reflected in the larger relaxivity of this complex in the absence of Ca^{2+}, but isolates the Gd centers from the effects of Ca^{2+} binding.

4.1.2. Luminescence

Several of the lanthanide ions having luminescence properties useful to the fields of microscopy and bioassay are emissive in the near-infrared frequencies [72]. They either absorb and emit light outside of the usual range of biomolecules (Nd^{3+} Er^{3+}, and Yb^{3+}), or have particularly long luminescent lifetimes (Eu^{3+} and Tb^{3+}). Faulkner et al., have studied these properties utilizing various linked azamacrocycle as ligands [21,22,73]. Ligand **72** was complexed to Yb^{3+}. Excitation at 337 nm represented energy transfer from the ligand to the Yb^{3+}, which resulted in a typical ytterbium-centered time-resolved emission spectrum [22]. Since the relative weighting of the short and long components of the decay were the same in both H_2O and D_2O, it was concluded that there must be two distinct environments for Yb^{3+}. Values of q (the number of bound water molecules) were determined to be 0.3 and 1.0 for these two environments. Apparently, the linking phenolate is shared unequally, as might be expected due to the bulky pendant-armed macrocycles preventing the close approach of both metal ions required for bridging by the phenolate oxygen.

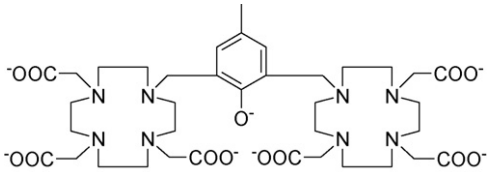

72

An interesting hetero-lanthanide complex was synthesized from **70**, in order to study Tb^{3+}-sensitized Yb^{3+} luminescence [73]. Tb^{3+} was complexed to the DOTA macrocycles, and the resulting complexes showed classic Tb^{3+} emission behavior and indicated that the two Tb^{3+} binding sites were identical. Subsequent complexation of Yb^{3+} to the DTPA-like linker gave the mixed lanthanide complex, where the kinetically inert macrocycles maintain their bound Tb^{3+}. The Yb^{3+} ion appears to have a coordination number of eight, all coming from the DTPA-like linker; q was calculated at 0.2 demonstrating little water interaction. Excitation of

the Tb^{3+} excitation band at 488 nm resulted in Yb^{3+} emission at 980 nm, the first use of one lanthanide as an antenna to excite another.

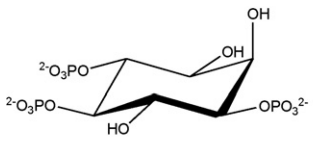

73 = IP_3

74 = CTP_3

Finally, ligand **65** was complexes to Eu^{3+}, Tb^{3+}, and Yb^{3+} in order to study their luminescent properties [21]. The aromatic linker, demonstrating similar absorptivity in the free ligand and in the complexes, was used as an antenna to increase the absorption properties of the complexes. The Eu^{3+} emission was clearly sensitized by the aromatic linker, although it was relatively weak due to non-radiative quenching of the LMCT state. Tb^{3+} likewise demonstrated efficient energy transfer, as emission was much stronger when the linker was excited (260 nm) than when the Tb^{3+} itself (366 nm) was excited. The **65** Yb^{3+} complex, unlike the **70** Yb^{3+} complex, demonstrated only one type of coordination environment. In fact, for all three lanthanides, both metal ions appeared to have the same coordination environment in both macrocycles. Interestingly, the lanthanide contraction was observed in the calculated value of q, which decreased from 2 to 1.4 to 0.4 for Eu^{3+}, Tb^{3+}, and Yb^{3+}, respectively.

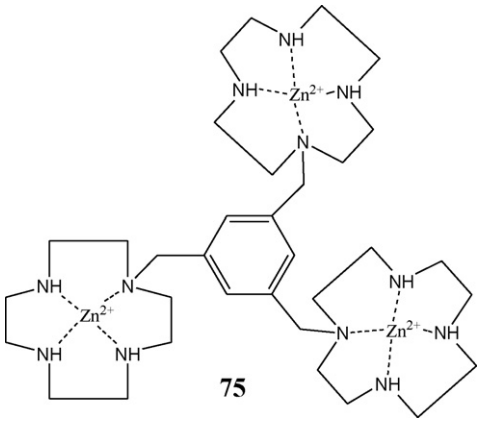

75

A structure similar to, but even more complex than **68** was used as a luminescence sensor for the important intracellular signal messenger Inositol 1,4,5-triphosphate (IP_3, **73**) [74]. Initially, **75** binding of achiral *cis*-1,3,5-cyclohexanetriol triphosphate (CTP_3, **74**) was studied prior to the more complicated system. Because the Zn^{2+} ions in **75** [74] and the phosphate groups in **74** should both be around 10 Å apart, a C_3-symmetric complex was envisioned. Potentiometric pH titrations revealed that a complex did form with an apparent complexation constant of $\log K = 8.0$. Based on this result, a new 2,2′-bipyridine linked azamacrocycle dimer **76** was synthesized [74] and used to assemble a sensor for IP_3 and CTP_3 (**G5**) based on the known $Ru(bpy)_3$ luminescent properties [75].

1:2 complex formation between **77** and **74** was observed by NMR titration and UV spectroscopic methods. Luminescence titrations revealed that addition of **74** to solutions of **77** results in a large increase (4.2-fold) in emission with a 26 nm blue shift. The enhancement is ascribed to conformational restriction of **77** upon **74** binding. Apparent binding constants calculated from potentiometric pH titrations were found to be $\log K = 30.6$ for the first CTP_3 to bind, and $\log K = 19.0$ for the second. Chiral IP_3 (**73**) addition (3 equiv.) studied by luminescence titration yielded a 2-fold increase in **77** emission with a similar blue shift. Achiral CTP_3 (**74**) added to this same solution resulted in further emission enhancement, suggesting that the chiral **73** cannot bind all of the stereoisomers of **77** present in solution. This indicates a high degree of enantioselectivity in **77**/**73** binding.

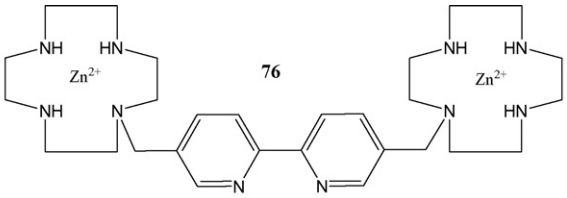

76

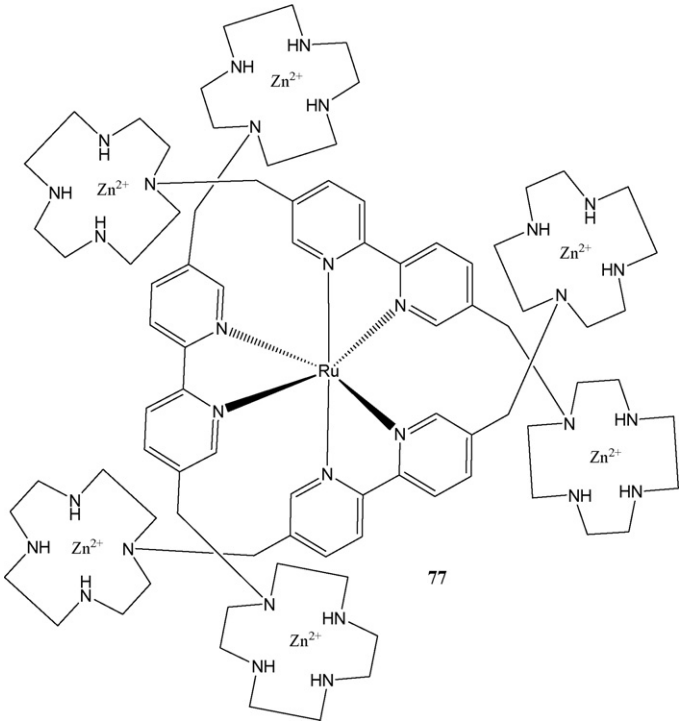

77

Another application of luminescent linked azamacrocycle complexes targets the medicinally important dicarboxylates [76]. The dinuclear Tb^{3+} complex of linked azamacrocycle **78** was designed to bind dicarboxylates, one functional group to each Tb, and use the xylene linker as an antenna to excite the Tb^{3+} ions [18]. In water, the Tb_2 complex was characterized as having two bound water molecules per Tb^{3+} ion, potentially labile sites to be replaced by chelating carboxylates.

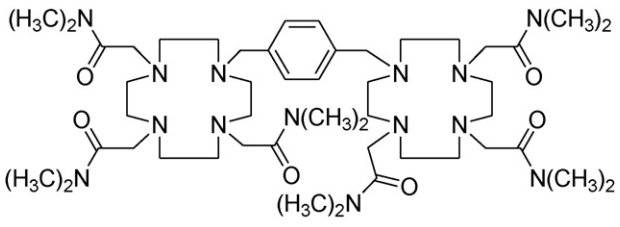

78

Excitation of the xylene linker resulted in emission from the Tb^{3+} ions, although quenching from the bound water molecules rendered the Tb^{3+} emission weak. Addition of monocarboxylate **79** resulted in **79** concentration dependent enhancement of Tb^{3+} emission, as **79** replaces the quenching water ligands, and acts as an antenna for Tb^{3+} excitation. Analysis of the fluorescent changes indicated that the Tb^{3+} ions were not communicating. Aromatic dicarboxylate **80** increased the emission of the complex 26-fold, with a maximum at 1:1 stoichiometry, indicating a bridging of the two Tb^{3+} ions by the dicarboxylate.

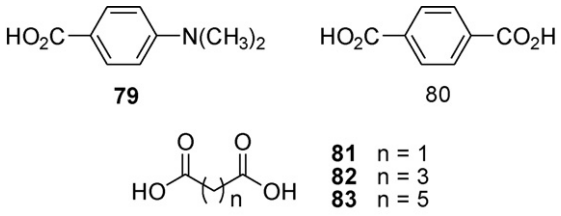

A range of aliphatic dicarboxylates (**81**–**83**) were also tested for binding and luminescence enhancement. The luminescence enhancement for these dicarboxylates was much less than for aromatic **79** and **80**, because they cannot act as antenna, leaving only the xylene linker to play this role. **81** formed a 2:1 complex, and is thus apparently too short to bridge both lanthanides. **83** formed a 1:1 complex, having the appropriate length to span both metal ions. Interestingly, **82** caused no changes to the luminescence, indicating the Tb_2**78** complex is somewhat selective toward dicarboxylate binding.

4.1.3. Radiolabelling

Research and clinical applications for macrocycles bound to radioactive isotopes, typically conjugated to antibodies or some other biomolecule, are becoming quite common [77]. Linked azamacrocycles, however, have only contributed to this application in small numbers. Two-ring (**84**) and three-ring (**85**) systems specifically designed for bioconjugation for radiolabelling studies have been reported [34,78]. In the initial report, only the syntheses of these linked azamacrocycles was reported. Very recently, [78] details regarding mAbs conjugation, ^{64}Cu interaction, and animal studies have appeared. 2:1 $^{64}Cu^{2+}$ complexation of **84a** > 95% was achieved at pH 5.0 after heating to 50 °C for 1 h. Even at pH 8.0, **85a** could bind only 83% of the possible $^{64}Cu^{2+}$ for 3:1 complexation. Once formed the **84a** 2:1 complex is quite stable in human serum, although the **85a** complex is less so, with loss of 20% of its $^{64}Cu^{2+}$ after 24 h incubation. This loss was attributed to the more weakly Cu-binding dioxocyclam central ring. 2:1 complexation of **85a** resulted in a much more stable complex, with only 2% loss of the radioisotope.

Conjugation of the 2:1 ^{64}Cu:ligand complex of **85b** to B72.3 mAb, which targets the Tag-72 antigen of colorectal and ovarian cancers, was carried out. Studies showed 2.7 ligands (or 5.5 $^{64}Cu^{2+}$) per mAb for this conjugate and the immunoreactivity was >80%. Finally, the tris-azamacrocycle **85b** mAb conjugate showed levels of accumulated radioactivity at the tumor similar to a mono-macrocycle analogue, but was able to reach this level with only about 70% of the antibody conjugate required, due to the presence of the second $^{64}Cu^{2+}$ binding site.

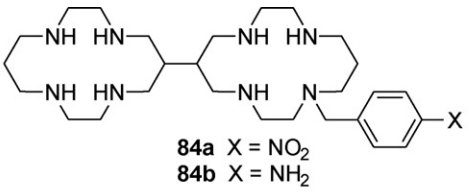

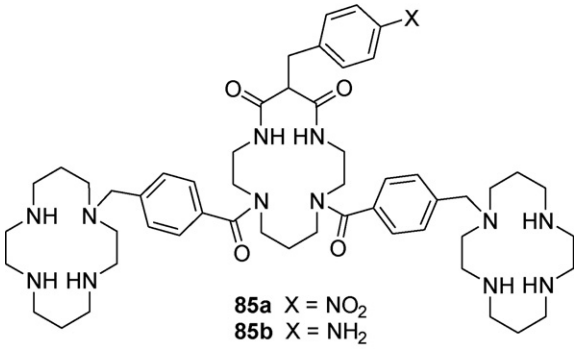

A large series of linked cross-bridged (**86**) and side-bridged (**87**) tetraazamacrocycles has been patented for radiolabelling applications in a collaboration involving one of the authors of this review [79]. Radiolabelling studies will be presented in the primary literature [80]. The ligands and transition metal complexes involved have also been applied as CXCR4 antagonists, and will be discussed in detail Section 4.4 below.

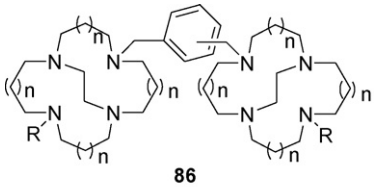

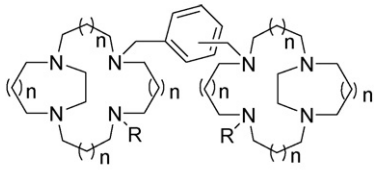

4.2. Binding DNA and its constituents

Kimura et al., have produced a number of papers describing linked $[Zn(cyclen)]_2^{2+}$ complexes that can efficiently bind biological molecules. Barbital was bound in a 1:1 complex with $\log K = 5.8$ at pH = 8 to a *para*-xylyl linked bis $Zn(cyclen)^{2+}$ complex **88** [81]. The 2:2 complex obtained at higher barbital concentration was actually crystallized and an X-ray crystal structure showed two barbital anions sandwiched between face-to-face **88** complexes. Molecular mechanics calculations confirmed that the 2:2 complex is 73.9 kJ/mol more stable than the 1:1 complex.

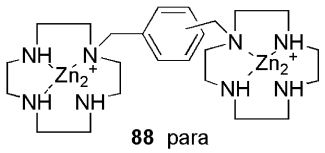

88 para
89 meta

The *meta* analogue **89** was published shortly thereafter, having a barbital binding constant of $\log K = 5.6$ at pH = 8 [82]. In this paper, it was noted that monomeric versions of **89** bind barbital only in a 1:1 fashion, whereas **89** has two macrocycle complexes (linked) per barbital. This "strong chelation" [82] effect increases the binding constant from $\log K = 4.9$ in the monomeric $Zn(cyclen)^{2+}$ analogue and allows for double deprotonation of barbital. Additionally, 4-nitrophenyl phosphate dianion binding was probe using **89** as a potential model of alkaline phosphatase [83], an enzyme having two Zn^{2+} cations at the catalytic center. A 1:1 affinity constant of $\log K = 4.0$ was determined, but no phosphatase activity was found.

Inspired by a crystal structure where three $Zn(cyclen)^{2+}$ complexes interact equivalently with the three unsubstituted oxygens of 4-nitrophenyl phosphate, Kimura et al., linked three $Zn(cyclen)^{2+}$ complexes through a mesitylene core (**75**) [84]. The likely C_3-symmetric linked azamacrocycle metal complex host, and its binding to a range of phosphate dianions was probed. Phenyl phosphate ($\log K = 6.6$), 4-nitrophenyl phosphate ($\log K = 5.8$), α-D-glucose-1-phosphate ($\log K = 7.0$), and phenyl phosphonate ($\log K = 7.9$) were all found to bind **75**. Use of the complex as a model for phosphatases that have three Zn^{2+} ions was also proposed.

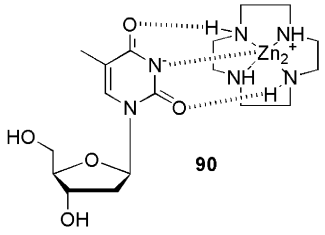

90

$Zn(cyclen)^{2+}$ binds thymidine highly efficiently ($\log K = 3.1$) [85], through zinc coordination to the deprotonated imide and cyclen NH to thymidine C=O hydrogen bonds (**90**). This observation has led to a number of studies involving linked azamacrocycle complexes. In an effort to prevent the UV photodamage of nucleic acids, **88** and **89** were studied for their effect on the photo[2 + 2]cycloaddition of thymidilyl(3′-5′)thymidine **91** and the photosplitting of the *cis-syn* cyclobutane thymine dimer **92** [86].

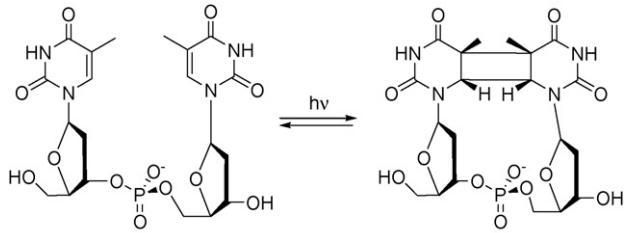

91 **92**

The affinity constants of **88** and **89** towards **91** were found to be identical within experimental error, at $\log K = 6.4$ for the 1:1 complexes. This value is about 1000 times greater than the affinity of the monomeric $Zn(cyclen)^{2+}$ 2:1 complex.

Compared to control reactions, **88** and **89** reduced the initial rates of the photodimerization reaction by 70% and 85%, respectively, with both complexes allowing ~90% of **91** to remain intact at equilibrium. Beginning with pure **92**, the reverse reaction was carried out in the presence of **89** and monomeric $Zn(cyclen)^{2+}$, independently. The dimeric complex was more efficient at returning **92** to an equilibrium mixture with **91** very similar to the one achieved in the forward reaction experiments. Finally, poly(dT) was photodimerized in the presence and absence of **89**. Not only did **89** reduce the equilibrium amount of photodamage (35% compared to 50% for the control), but addition of **89** to a control reaction at equilibrium returned the sample to lower levels of photodamage, indicating that **89** is actually capable of promoting photodamage repair.

The thymidine dimer (TpT) interaction with **88** was examined in the same publication in which a linearly arranged trimer of $Zn(cyclen)^{2+}$ complexes linked by *para*-xylyl groups (**93**) was synthesized and interacted with the thymidine trimer (TpTpT) [87]. UV titration confirmed that 1:1 complexes of TpT with **88** and TpTpT with **93** were formed in aqueous solution. The TpT dimer–**88** interaction, from NMR measurements, appears to use the same binding motif as in **90**, with $\log K = -5.5$ obtained from potentiometric pH titrations. An even more impressive $\log K = -6.4$ was determined for the TpTpT–**93** complex. Overall 1:1 affinities for **90** ($K_d = 0.079$ mM), TpT–**88** ($K_d = 0.63$ μM), and TpTpT–**93** ($K_d = 0.80$ nM) species are perhaps most useful for comparison.

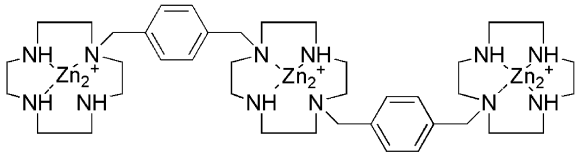

93

Because several anti-HIV reverse transcriptase inhibitors (AZT = 3′-azido-3′-deoxythymidine, ddC = 2′,3′-dideoxycytidine, ddA = 2′,3′-dideoxyadenosine) [88] must undergo phosphorylation to triphosphate derivatives to be activated inside the cell, lipophilic carrier molecules for the nucleotide phosphates would be medicinally useful [89]. Combining their knowledge of the binding ability for nucleotides already discussed with the evidence that $Zn(cyclen)^{2+}$ binds dianionic phosphates [84], Kimura et al., decided to evaluate their linked azamacrocycle systems **88** and **89** with respect to a number of thymidine, uridine, and AZT phosphorylated nucleotides [90]. Due to the additional interaction of the phosphate group with the second $Zn(cyclen)^{2+}$ moiety, apparent binding constants with **88** and **89** were up to 1000 times higher than for the same phosphorylated nucleotides with monomeric $Zn(cyclen)^{2+}$, with the *para* isomer typically slightly better than the *meta* isomer. The selectivity of these linked azamacrocycle complexes for dT(U) nucleotides and the possibility of lipophilic functionality attachment to produce novel drug transport agents was noted [90].

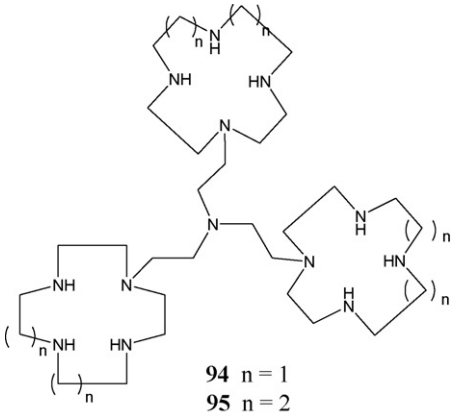

94 n = 1
95 n = 2

A natural progression for the nucleotide-binding agents **88**, **89**, **75**, and **93** was to explore their effects on double-stranded DNA [91]. Melting studies of double-stranded polymers revealed **88** and **93** to completely denature 50 μM nucleobase poly(dA)·poly(dT) at

25 °C at concentrations of 4 and 2.5 μM, respectively. Complete denaturation of poly(dA-dT)$_2$ under the same conditions by **88** and **93** occurred at concentrations of 7 μM and 4 μM, respectively. Selective binding of **88**–**89**, **75**, and **93** to poly(dT) was examined using a micrococcal nuclease footprinting assay of a 150-bp DNA fragment. The poly(dT) regions were particularly well protected from hydrolysis, while poly(dA) regions on the complementary strand were made more susceptible to hydrolysis. IC_{50} (inhibitory concentration) values against the nuclease were found to be much lower (0.5–6 μM) than for the monomeric Zn(cyclen)$^{2+}$ complex (>100 μM). The most effective compound in this assay (0.5 μM) was **93**. Binding constants for **93** were determined as $K = 2.1 \times 10^8\ M^{-1}$ with poly(dA)·poly(dT) and $K = 4.7 \times 10^7\ M^{-1}$ with poly(dA-dT)$_2$. These values suggest that **93** binds to the poly(dT) sequence in double-stranded DNA as strongly as the known minor groove binder Distamycin A [92].

4.3. Catalysis

4.3.1. Ester cleavage

Tren-based linked azamacrocycle complex trimers [93] have been used to mimic the active site of multinuclear metalloenzymes, such as P1 nucleases, which use three metal ions to cleave nucleotide phosphate esters [94]. The ligands **94** and **95** are C_3-symmetric, like **75**, but are more flexible due to the tren-based linker compared to the aromatic core of **75**. The Zn_3 complexes of **94** and **95** were examined as hydrolytic agents using the activated ester **96** and the activated phosphate ester **97** [93a]. Hydrolysis of ester **96** was pH dependent, with little activity at low pH due to hydroxo ligands bridging between Zn^{2+} ions. At higher pH's when bridging is not observed, hydrolysis increases. The **94** complex exhibits a second order rate constant of $k' = 4.2\ M^{-1}\ s^{-1}$ compared to the **95** complex value of $k' = 3.7\ M^{-1}\ s^{-1}$. Both of the values are much higher than the mononuclear Zn(cyclen)$^{2+}$ rate constant $k' = 0.11\ M^{-1}\ s^{-1}$ [95]. The authors observe that "... the rate constants increase with the pK_a value, i.e. with the nucleophilicity of the Zn–OH functions" [93a]. The Zn^{2+} ions do not appear to cooperate, and the typical bimolecular mechanism is observed.

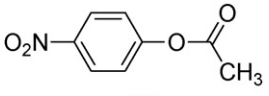

96

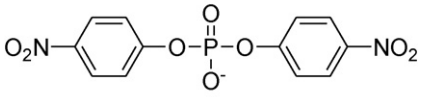

97

Phosphate ester hydrolysis using **97** follows similar pH dependence, but the rate is much enhanced. Five- and 14-fold rate enhancements are observed for the zinc complexes of **94** ($k' = 1.1 \times 10^4\ M^{-1}\ s^{-1}$) and **95** ($k' = 3.1 \times 10^4\ M^{-1}\ s^{-1}$), respectively, vs. the mononuclear Zn(cyclen)$^{2+}$ rate constant $k' = 0.21 \times 10^4\ M^{-1}\ s^{-1}$ [95]. This result suggest the metal centers are cooperating in this case. A mechanism is proposed by which the substrate phosphate bridges two of the Zn^{2+} cations prior to hydrolytic attack from one of the bound hydroxo groups. Evidence for this mechanism is found in that the hydrolytic ability decreases as the pK_a of the complex increases. This is the opposite behavior as found for the ester case, suggesting an associative cleavage mechanism. The trinuclear Cu^{2+} complex of **94** was prepared and tested for its effect on **97** hydrolysis, as well [93b]. A pseudo-first order rate constant for the Cu_3**94** complex of $k = 3.5 \times 10^6\ s^{-1}$ was determined, which was declared "not particularly efficient" [93b]. Apparently, this complex does not form the desired hydroxo complexes, which are often the active species in **97** hydrolysis.

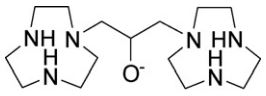

98

Cleavage of phosphodiesters and other RNA analogues by the di-zinc complex of **98** has been thoroughly studied in recent years [29,96]. Initial studies [96a] with **99** as the substrate resulted in the calculation of an observed $k_{cat} = 4.1 \times 10^{-3}\ s^{-1}$ at pH = 7.6 which makes this complex one of the most active dinuclear metal ion phosphodiester cleavage catalysts identified. Mechanistic insight gained by this study included the likely direct proton transfer from the C2-hydroxyl of the substrate to the catalyst, and the cooperative role of the two metal ions in stabilizing the transition state for the catalyzed reaction. Cleavage by Zn_2**98** of an oligoribonucleotide made of six adenosines resulted in 90% cleavage after 24 h [29], proving that the catalyst is not effective only on the activated **99** ester.

Comparison of the cleavage of "minimal" substrate **99** to a larger nucleoside substrate **100** showed that the catalyst was 50 times faster at catalyzing the hydrolysis of smaller **99** than of larger **100** [96b]. Hydroxide ion catalyzed cleavage of **100** is 10,000 faster than for **99**, due to several cumulative structural effects. The surprising decrease in activity for Zn_2**98** was ascribed to steric effects that potentially restrict access to the catalytic core of Zn_2**98**.

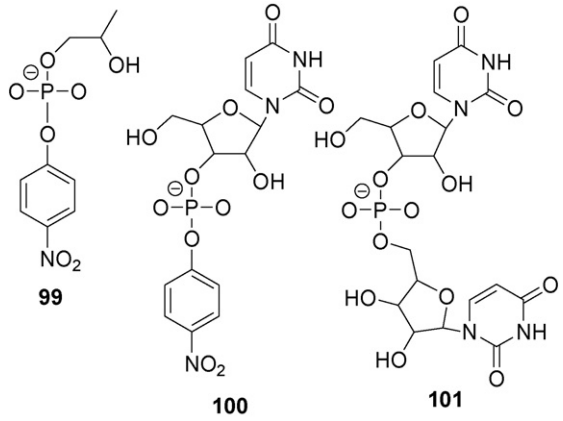

99 **100** **101**

Changing the metal ions complexed to **98** from Zn^{2+} to Cu^{2+} and Cd^{2+} was carried out, along with an analysis of how this affected the catalytic nature of the resulting complexes [96c]. Cd^{2+} appears to prefer to make a mononuclear complex with **98** until the pH is raised to above pH = 10, with only the dinuclear complex having significant activity towards **99** cleavage. However, once formed at high pH, the Cd_2**98** complex is about 5 times more active than the Zn_2**98** complex, possibly due only to the higher basicity of the Cd^{2+} bound hydroxide ion. Another possible explanation is that the larger Cd^{2+} ions are more sterically available, and thus more reactive, than in the Zn complex. The dinuclear Cu_2**98** complex is a poor catalyst (165 times slower than Zn_2**98**), most likely due to a lack of coordination sites for the substrate and the required hydroxide ligand, as Cu^{2+} is five coordinate in the complex according to X-ray crystal structure data [97].

Solvent deuterium isotope effects were explored for Zn_2**98** catalysis of **100** [96d], since a concerted movement of a proton at the rate-determining transition state is signaled by faster cleavage of phosphodiesters in H_2O than in D_2O [98]. The possible kinetic primary solvent deuterium isotope effect was not observed. Con-

clusions from the study were that there is no movement of the proton at the rate-determining transition state, and therefore, no significant transition state stabilization due to concerted proton transfer. The major implication for the catalyst mechanism is that the observed rate acceleration must be due primarily to interaction of the dianionic transition state with the two metal dications. The authors conclude: "These results illustrate the power of simple electrostatics in small molecule catalysis of phosphate diester cleavage . . ."

Extension of the study of Zn_2**98** phosphate diester cleavage was finally extended to a ribodinucleotide substrate **101** that would have the same leaving group as RNA [96e]. It was conjectured that an enhanced rate acceleration might be observed, due to a likely stabilization of the strongly basic anion leaving group by the densely charged catalyst. In previously studied **99** and **100**, the leaving group is a weakly basic 4-nitrophenoxide anion. In fact, this altered electrostatic interaction was observed, and was characterized as a 2.1 kcal/mol greater stabilization of the transition state for **101** cleavage, than for **100** cleavage. However, the desired rate enhancement was not realized, as the stronger transition state interaction apparently slows the overall catalytic rate.

A number or linked azamacrocycle zinc complexes using 1,5,9-triazacyclododecane have been evaluated as phosphate diester catalysts [43]. Monomer Zn(1,5,9-triazacyclododecane)$^{2+}$ cleavage of **101** is only enhanced slightly by the dimer complexes **102**–**107**. However the trimer complex **107** accelerates this cleavage rate to 50 times that of its dimeric analogue **103**. The proposed explanation for this observation is that the dimeric complexes coordinate their Zn^{2+} ions to each of the uracil bases of **101** in a similar manner to thymidine binding to Zn(cyclen)$^{2+}$ **90**. The central phosphate ester is not, therefore, directly engaged by either metal ion for cleavage. However, the trimer complex **107** can bind the two uracil bases and still interact with the phosphate ester for cleavage with the third Zn^{2+} complex. If either of the uracil bases of **101** is replaced by adenine, which cannot bind efficiently to the Zn(1,5,9-triazacyclododecane)$^{2+}$ complex, cleavage is up to 100 times faster with the dimer complexes of **102**–**106** than cleavage of **101**. Now, strongly binding one Zn^{2+} complex to the lone uracil helps place the other linked Zn^{2+} complex in position to effectively cleave the phosphate ester.

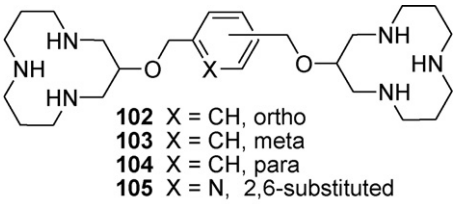

102 X = CH, ortho
103 X = CH, meta
104 X = CH, para
105 X = N, 2,6-substituted

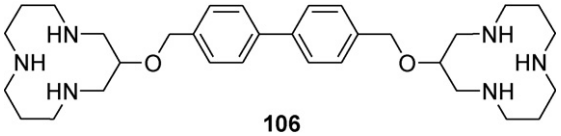

106

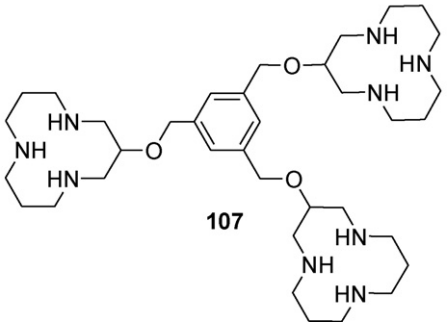

107

The effect of reduced solvent polarity on the cleavage rate of **99** by the zinc complex of a linked azamacrocycle has recently been probed [99]. The catalyst examined uses the same macrocycle as **102**–**107**, but only a propylene linker (**108**). Enzyme active sites may be considered "non-aqueous" [100]. Thus, enhancing electrostatic interactions between substrate and catalyst by studying the reaction in a solvent like methanol may lead to enhanced reaction rates. Indeed, acceleration of the reaction rate in methanol for the monomer Zn(1,5,9-triazacyclododecane)$^{2+}$ by 1000 times the analogous aqueous rate was observed, which is also 6500 faster than methoxide alone. A truly remarkable rate enhancement is observed with the dimer complex of **108**. The rate is now 1.1×10^8 times faster than methoxide alone and several orders of magnitude faster than any previously reported catalytic cleavage of **99** [99b]. Strikingly, the reactivity of Zn_2**108** in water is not any greater than monomeric Zn(1,5,9-triazacyclododecane)$^{2+}$ [101], demonstrating that solvent effects are indeed important.

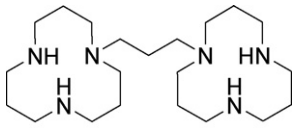

108

Recent experiments with the same catalyst cleaving DNA model methyl *p*-nitrophenyl phosphate in aqueous ethanol [102] shows rate acceleration of this reaction (a factor 1.6×10^{17} relative to background OH^- promoted reaction). This work demonstrates that control of solvent in addition to the use of linked azamacrocycle complex catalysts can produce enzyme-like catalytic rates.

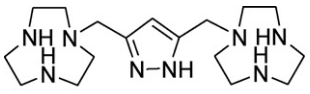

109

Another linked azamacrocycle used to produce hydrolytic catalyst complexes is **109** [103]. Cleavage of substrate **97** to produce 4-nitrophenylphosphate was observed by NMR for the Zn^{2+} complex. Copper(II), nickel(II), and zinc(II) complexes were all then evaluated spectrophotometrically for **97** cleavage kinetics. Interestingly, the Ni^{2+} complex was about 50 times more active than Zn^{2+}, and the Cu^{2+} complex did not show any rate enhancement of the reaction. It was speculated that perhaps not enough coordination sites are available in the dicopper complex for catalysis to occur. The larger rate enhancement for the Ni^{2+} complex was explained by the fact that a OH^- coordinated to Ni^{2+} is more basic than when bound to Zn^{2+}, a fact that agreed with the proposed catalytic mechanism.

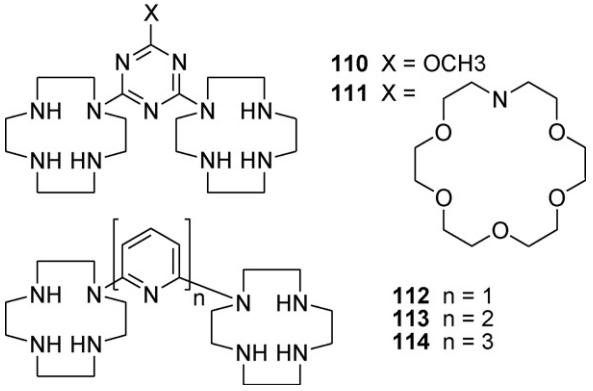

110 X = OCH_3
111 X =

112 n = 1
113 n = 2
114 n = 3

Triazine (**110**, **111**) and polypyridine (**112**–**114**) linked cyclen ligands have been developed for catalytic ester hydrolysis studies as well [104]. The zinc complex of **110** was crystallized and

exhibits a structure where the two Zn^{2+} ions are coordinated to only the three secondary nitrogens of each cyclen and are bridged by a OH^- ion, which may be an active participant in ester hydrolysis. All Zn^{2+} complexes enhance the hydrolysis of carboxylic ester **96** under physiological conditions [104a]. Under the studied conditions, $Zn(cyclen)^{2+}$ exhibited a rate constant for **96** hydrolysis of $k_{cat} = 106\ M^{-1}\ s^{-1}$. The monohydroxo species of di- and tri-pyridyl linked complexes of **113** and **114** gave k_{cat} values of 7170 and $7860\ M^{-1}\ s^{-1}$, respectively. The shorter linked ligands **110**–**112** performed somewhat better, with k_{cat} values of 41,000, 31,000, and $44{,}000\ M^{-1}\ s^{-1}$, respectively. These latter values are very similar to the activity of tren-based Zn_3**94**, which had a k_{cat} value of $42{,}000\ M^{-1}\ s^{-1}$ [93]. However, it was pointed out that these complexes perform somewhat better at physiological pH than does Zn_3**94**. The crown-ether functionality of **111** appears to impart some steric crowding, which may explain the somewhat smaller activity.

Phosphodiester cleavage of these complexes was evaluated using **97** as the substrate [104b]. At pH = 8, the second order rate constants for the Zn_2 complexes of **110**, **111**, and **113** were found to be 1.28×10^{-3}, 2.45×10^{-3}, and $0.244 \times 10^{-3}\ M^{-1}\ s^{-1}$, respectively. These values are 100–1000 times faster than the reactions catalyzed by the monomeric analogues [104b]. The longer linker of **113** appears to be disadvantageous to phosphate ester cleavage, as it was in carboxylic ester cleavage (*vide supra*). The **110** and **111** catalysts are 1–2 orders of magnitude more active than the previously discussed catalyst Zn_3**94** at pH = 8 [105], making these complexes better suited for phosphate ester hydrolysis under physiological conditions.

4.3.2. Other catalytic reactions

Catalytic diproportionation of H_2O_2 was the goal behind the synthesis of a series of linked triazacyclononanes having 2-pyridylmethyl pendant arms [106]. A range of linking groups was utilized to produce ligands **115**–**119** for Mn^{2+} complexation. These ligands increase the denticity of the triazacyclononanes for better complex stability, and the pyridine donors might be expected to help stabilize higher oxidation states of Mn. X-ray crystal structures of the Mn^{2+} complexes of **115**–**117**, as well as the monomeric ligand analog, were obtained, and all showed pentacoordination of the pendant-armed macrocycle plus a single chloride ligand. Addition of excess H_2O_2 to DMF solutions of these complexes resulted in color changes, as well as the evolution of dioxygen. Coordinative saturation was expected to preclude this type of reactivity, as most Mn catalysts of this reaction were known to be μ-oxo dimers of tridentate ligands [107]. Electrochemical and EPR experiments suggested that the complex of ligand **119** likely forms an endogenous propoxide bridge, which makes its electrochemical behavior unique. The **115** complex alone exhibited EPR behavior most likely due to dissociation of some N-donors and bridging by exogenous O donors. Unfortunately, precipitation of MnO_2 during the H_2O_2 reaction with all complexes indicated that the complexes decompose during the catalytic process.

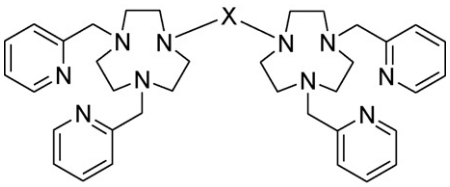

115 X = CH_2CH_2
116 X = $CH_2CH_2CH_2$
117 X = $CH_2CH_2CH_2CH_2$
118 X = *m*-xylyl
119 X = $CH_2CH(OH)CH_2$

A linked cyclam ligand (**120**) using the same 2-hydroxypropane linker as **98** and **119** has recently been used to make manganese and iron complexes also studied as hydrogen peroxide disproportionation catalysts [27]. X-ray crystal structures with both Mn and Fe show the propoxide oxygen acting as a bridging ligand between cyclam bound metal ions. EPR measurements in an acetonitrile water solvent mixture confirm that the Mn^{2+} ions are still bridged in an aqueous environment. A turnover number in the reaction of the Mn_2**120** complex with H_2O_2 in water of 20,000 was reported, and consistent catalase activity is reported for over an hour after H_2O_2 addition. The cyclam macrocycles appear better able than **115**–**119** to stabilize the likely high oxidation state manganese ions produced during the catalytic cycle without decomposition. The iron complex of **120** was not an active catalyst for H_2O_2 decomposition. Efforts to isolate higher oxidation state complexes of both metal ions are ongoing.

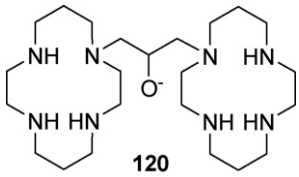

120

Ni(cyclam)$^{2+}$'s success in the catalytic reduction of CO_2 to CO [108] spurred the study of a number of linked azamacrocycle systems (**121**–**129**) for similar reactivity [109]. The presence of two nickel ions was hoped to result in the reduction of CO_2 beyond CO. The catalytic reduction of CO_2 with the surface-confined dinickel complexes of ligands **121**–**129** was evaluated using a mercury-coated silver electrode under CO_2 gas. Interestingly, the dinuclear pentaaza complexes' catalytic currents were only about half of the value for a mononuclear analogue. The conclusion from this result is that only one nickel site per dimer is adsorbing on the electrode, and is thus able to maintain catalytic activity. The more rigid, planar **125** complex had the largest catalytic current, likely because its structure most favored both nickel centers achieving planarity on the electrode.

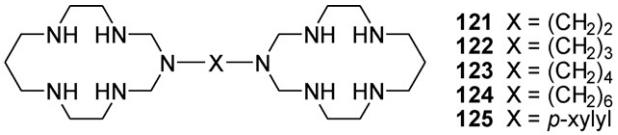

121 X = $(CH_2)_2$
122 X = $(CH_2)_3$
123 X = $(CH_2)_4$
124 X = $(CH_2)_6$
125 X = *p*-xylyl

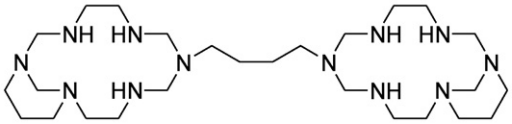

126

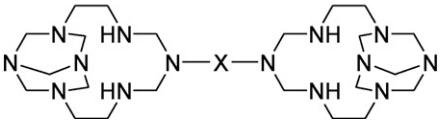

127 X = $(CH_2)_2$
128 X = $(CH_2)_3$
129 X = $(CH_2)_5$

The catalytic current for the complexes of **121**–**124** increased with the length of the linker, which was attributed to greater flexibility allowing both nickel sites better interaction with the electrode surface. Bulk CO_2 electrolysis and product analysis was carried out only on the complex of **123**. CO_2 and H_2 were the major products detected. After about 10% of the available CO_2 was reduced to CO, changes in current and product distribution corresponded with deactivation of the catalyst due to nickel deposition.

The dinickel complex of **126** was a poor catalyst for CO_2 reduction having a catalytic current about 15% of the pentaaza complexes, perhaps due to the additional steric hindrance. The tetraazabicyclononane fragment of ligands **127**–**129** occupies the

same space around Ni^{2+} as ethylenediamine. Therefore, these ligands can be thought of as acting as 13-membered macrocycles around Ni^{2+}. These sterically hindered **127**–**129** complexes were also relatively poor catalysts, with catalytic currents only about 10% of the pentaaza complexes. As was the case for **121**–**124**, the catalytic current did increase with chain length (i.e. flexibility) for the complexes of **127**–**129**.

4.4. CXCR4 antagonists

Due to the important place CXCR4 antagonist linked azamacrocycle and their metal complexes hold in the medicinal chemistry of several diseases [44–55] (see Section 3.1 above) comprehensive reviews devoted to these medicinal applications are periodically published [44]. Reviews detailing the early development of the organic molecules [44b,110], discovery and exploration of the effect of metal complexation [111], and recent state of the art [44], cover this broad area of active chemical and biological research so well as not to need replication here. Instead, we have chosen to focus on only the most recent findings regarding linked azamacrocycle metal complexes and their interaction with the CXCR4 receptor. In particular, the recent work on linked *bridged* azamacrocycle complexes published by one of us in collaboration with Archibald and De Clercq will be highlighted.

Bridger, Sadler, and De Clercq were instrumental in defining the importance of metal ion binding to linked azamacrocycles like AMD3100 (**45**). Metal complexes of **45** were first tested against HIV in 1999, when an order of activity of $Zn^{2+} > Ni^{2+} =$ **45** $> Cu^{2+} > Co^{3+} > Pd^{2+}$ was identified [51c]. $Zn(cyclam)^{2+}$ and Zn_2**45** complexes studied by X-ray crystallography and NMR have revealed that multiple configurations of the macrocycle around Zn^{2+} are possible and likely in equilibrium in aqueous solution [112]. Acetate binding [112], as a model for aspartate in CXCR4 [49] (see Section 3.1) results in the increase in concentration of the *cis*-V configuration, as chelation of the carboxylate group likely occurs. An X-ray crystal structure of Zn_2**45**$(OAc)_4$ shows this configuration for both metal centers [112a].

There is evidence that interaction through only one metal ion to Asp262 for **45** complexes is sufficient to explain the enhanced binding over **45** alone [113]. The nature of the binding interaction with Asp171 is not as clear, although nothing has ruled out carboxylate coordination by the second metal ion of **45** complexes. CXCR4 docking studies employing configurations for the two Zn-cyclam complexes of Zn_2**45** of *cis*-V/*trans*-I [112a] and *trans*-III/*trans*-III [114] have been independently performed, both of which strongly suggest metal coordination of both metal ions is important.

Our recent work in this area has centered on the synthesis and evaluation of the CXCR4 binding properties of a series of configurationally restricted analogues of **45**. If metal ion complexation to the aspartate residues is important, the configuration of the macrocycle around the metal ion is critical as well (Fig. 4). Controlling the configuration could easily improve the binding efficiency of potential drug molecules, by pre-organizing the complex into the preferred binding geometry prior to interaction with the aspartate carboxylates. A strategy to select for specific configurations is to add an additional ethylene bridge between nitrogen atoms of the cyclam rings of **45**, as in **130** (side-bridged) and **131** (cross-bridged). The side-bridged cyclam complexes adopts only the *trans*-II configuration when the macrocycle is mono-alkylated [13a,115]. The cross-bridged cyclam is topologically constrained to the *cis*-V configuration in its transition metal complexes [13b,116]. Linked bridged azamacrocycles **132** and **133** have been prepared, and their Cu^{2+} and Zn^{2+} complexes tested for CXCR4 binding ability and anti-HIV activity [13,79,115].

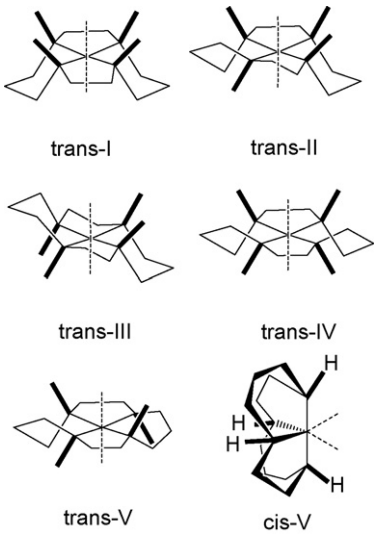

Fig. 4. The six possible configurations of cyclam in its metal complexes.

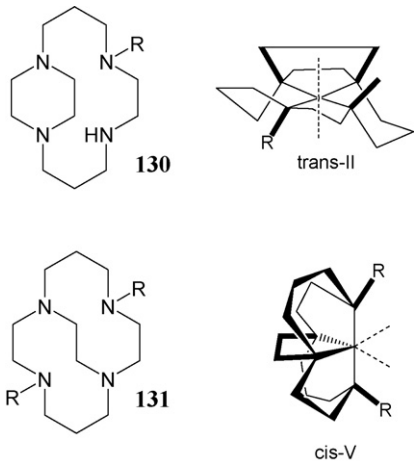

Our initial report [13a] focused on Zn_2**132**, its crystal structure with bound acetate anions, and its anti-HIV activity. In the solid state, both side-bridged cyclams are in *trans*-II configurations around Zn^{2+} with the acetate ligands bound to each Zn^{2+} in an anisobidentate fashion. High-field NMR studies showed only one configuration in aqueous solution, as well, which differs from the Zn_2**45** complex, which shows multiple configurations in equilibrium [112a]. The Zn_2**132** complex was shown to bind CXCR4 by flow cytometry displacement studies with an anti-CXCR4 antibody. In identical studies for infection of HIV-1(III_B) in MT4 cells, the EC_{50} (average effective concentration) of Zn_2**132**, **45**, and Zn_2**45** were determined as 0.0025, 0.011, and 0.008 μM, respectively. Clearly, the *trans*-II restricted Zn_2**132** is at least as active as the configurationally unrestricted Zn_2**45** complex, reflecting the relevance of configurational restriction to the optimization of CXCR4 binding. The Cu_2**132** complex was found to be likewise more active than its Cu_2**45** counterpart, with EC_{50} values measured as 0.026 and 0.047 μM, respectively [115a]. As previously observed for **45** complexes [51c], the Cu^{2+} was not as active against HIV as the Zn^{2+} complex, in this case by about an order of magnitude.

In our most recent work, we have demonstrated that Cu^{2+} complexes can, in fact, be as active against HIV as Zn^{2+} complexes [13b]. Cu_2**133** did not yield usable crystals, but a monomeric analogue using **131** having one methyl and one benzyl R group, did. The complex Cu**131**(OAc) has a distorted square pyramidal geometry around a Cu^{2+} ion bound to all four nitrogens of the macrocycle and

only one of the acetate oxygens. The azamacrocycle is forced into a *cis*-V configuration by the ethylene bridge. Importantly, the bound acetate oxygen is forming a shorter equatorial bond rather than the longer axial bond that would be available in the most common configuration for $Cu(cyclam)^{2+}$ complexes: *trans*-III. If the same structure is present for the **133** Cu^{2+} complex, binding to aspartate in CXCR4 (modeled by acetate here) would be expected to be shorter and stronger than in an unbridged ligand complex, such as **45**.

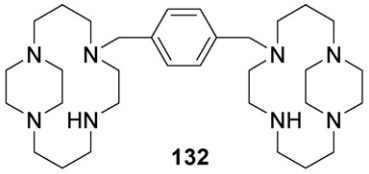

132

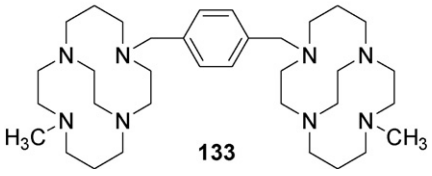

133

Evidence of this stronger binding is found in the EC_{50} value of the Cu_2**133** complex: 0.0042 μM. This value is nearly as good as the Zn_2**132** complex (0.0025 μM) and better than the Zn_2**45** complex (0.008 μM). Additional evidence of strong binding to CXCR4 was provided by flow cytometry displacement studies with an anti-CXCR4 antibody over the period of 4 days, after only one dose of the CXCR4 antagonist. Cu_2**133** retained a significant amount of antibody binding inhibition 96 h after dosing, whereas **45** and Cu_2**45** showed no inhibition after 48 h.

5. Conclusions

This review of recent syntheses and applications demonstrates that the future of linked azamacrocycles is bright. New methods to make these interesting molecules have been found, leading to a large number of new systems. Important chemical, biological, and medicinal problems have been assaulted using linked azamacrocycles and their metal complexes as useful tools, with significant advances made in a number of these areas. It is our perspective that these trends will continue and even intensify, with linked azamacrocycles assuming an ever more important role in chemistry.

Acknowledgements

TJH acknowledges the support of OK-INBRE, NIH, and the Research Corporation in his study of linked azamacrocycles.

References

[1] (a) A. Baeyer, Chem. Ber. 19 (1886) 2184;
(b) P. Rothemund, C.L. Gage, J. Am. Chem. Soc. 77 (1955) 3340;
(c) C.C. Leznoff, A.B.P. Lever (Eds.), Phthalocyanines, vol. 1–4, Wiley-Interscience, 1997, and references therein.
[2] (a) N.F. Curtis, J. Chem. Soc. (1960) 4409;
(b) N.F. Curtis, D.A. House, Chem. Ind. (1961) 1708.
[3] (a) C.J. Pederson, J. Am. Chem. Soc. 89 (1967) 2495;
(b) C.J. Pederson, J. Am. Chem. Soc. 89 (1967) 7017;
(c) C.J. Pederson, Aldrichim. Acta 4 (1971) 1.
[4] (a) D.A. House, N.F. Curtis, J. Am. Chem. Soc. 84 (1962) 3248;
(b) M.C. Thompson, D.H. Busch, J. Am. Chem. Soc. 84 (1962) 1762;
(c) M.C. Thompson, D.H. Busch, J. Am. Chem. Soc. 86 (1964) 213;
(d) M.C. Thompson, D.H. Busch, J. Am. Chem. Soc. 86 (1964) 3651.
[5] (a) L.F. Lindoy, The Chemistry of Macrocyclic Ligand Complexes, Cambridge University Press, Cambridge, 1989;
(b) J.S. Bradshaw, K.E. Krakowiak, R.M. Izatt, Aza-Crown Macrocycles, Wiley and Sons, New York, 1993.;
(c) K. Gloe, Macrocyclic Chemistry: Current Trends and Future, Springer, Dordrecht, 2005.
[6] (a) A. McAuley, S. Subramanian, Coord. Chem. Rev. 200–202 (2000) 75;
(b) T.A. Kaden, Coord. Chem. Rev. 190–192 (1999) 371;
(c) L.F. Lindoy, Coord. Chem. Rev. 174 (1998) 327.
[7] (a) J.D. Chartres, L.F. Lindoy, G.V. Meehan, Coord. Chem. Rev. 216–217 (2001) 249;
(b) L.F. Lindoy, Adv. Inorg. Chem. 45 (1998) 75.
[8] (a) A. Domenech, E. Garcia-Espana, N. Bernier, R. Tripier, H. Handel, Dalton Trans. (2008) 3169;
(b) F.H. Fry, B. Moubaraki, K.S. Murray, L. Spiccia, M. Warren, B. Skelton, A.H. White, Dalton Trans. (2003) 866;
(c) B. Graham, M.J. Grannas, M.T.W. Hearn, C.M. Kepert, L. Spiccia, B.W. Skelton, A.H. White, Inorg. Chem. 39 (2000) 1092;
(d) Y. Dong, L.F. Lindoy, P. Turner, G. Wei, Dalton Trans. (2004) 1264;
(e) S. El Ghachtouli, C. Cadio, I. Dechamps-Olivier, F. Chuburu, M. Aplincourt, T. Roisnel, V. Turcry, V. Patinec, M. Le Baccon, H. Handel, Inorg. Chem. 47 (2008) 4735;
(f) S. El Ghachtouli, C. Cadiou, I. Dechamps-Olivier, F. Chuburu, M. Aplincourt, V. Turcry, M. Le Baccon, H. Handel, Inorg. Chem. 44 (2005) 2658;
(g) M. Soibinet, I. Dechamps-Olovier, E. Guillon, J.-P. Barbier, M. Aplincourt, F. Chuburu, M. Le Baccon, H. Handel, Polyhedron 24 (2005) 143;
(h) M. Soibinet, I. Dechamps-Olivier, E. Guillon, J.-P. Barbier, M. Aplincourt, F. Chuburu, M. Le Baccon, H. Handel, Inorg. Chem. 42 (2003) 1984;
(i) K.T. Szacilowski, P. Xie, A.Y.S. Malkhasian, M.J. Heeg, M.Y. Udugala-Ganehenege, L.E. Wenger, J.F. Endicott, Inorg. Chem. 44 (2005) 6019;
(j) K. Mochizuki, K. Kashima, T. Weyhermüller, Inorg. Chem. Commun. 9 (2006) 891.
[9] M. Le Baccon, F. Chuburu, L. Toupet, H. Handel, M. Soibinet, I. Déschamps-Olivier, J.-P. Barbier, M. Aplincourt, New J. Chem. 25 (2001) 1168.
[10] G.R. Weisman, S.C.H. Ho, V. Johnson, Tetrahedron Lett. 21 (1980) 335.
[11] N. Bernier, R. Tripier, V. Patinec, M. Le Baccon, H. Handel, C. R. Chim. 10 (2007) 832.
[12] G.R. Weisman, M.E. Rogers, E.H. Wong, J.P. Jasinski, E.S. Paight, J. Am. Chem. Soc. 112 (1990) 8064.
[13] (a) G.C. Valks, G. McRobbie, E. Lewis, T.J. Hubin, T.M. Hunter, P.J. Sadler, C. Pannecouque, E. De Clercq, S.J. Archibald, J. Med. Chem. 49 (2006) 6162;
(b) A. Khan, G. Nicholson, J. Greenman, L. Madden, G. McRobbie, C. Pannecouque, E. De Clercq, R. Ullom, D.L. Maples, R.D. Maples, J.D. Silversides, T.J. Hubin, S.J. Archibald, J. Am. Chem. Soc. 131 (2009) 3416.
[14] A.D. Averin, A.V. Shukhaev, A.K. Buryak, F. Denat, R. Guilard, I.P. Beletskaya, Tetrahedron Lett. 49 (2008) 3950.
[15] J.P. Wolfe, S.L. Buchwald, J. Org. Chem. 65 (2000) 1144.
[16] J. Costa, E. Balogh, V. Turcry, R. Tripier, M. Le Baccon, F. Chuburu, H. Handel, L. Helm, É. Tóth, A. Merbach, Chem. Eur. J. 12 (2006) 6841.
[17] T. Gunnlaugsson, J.P. Leonard, S. Mulready, M. Nieuwenhuyzen, Tetrahedron 60 (2004) 105.
[18] A.J. Harte, P. Jensen, S. Plush, P.E. Kruger, T. Gunnlaugsson, Inorg. Chem. 45 (2006) 9465.
[19] T. Gunnlaugsson, A. Harte, J. Org. Biomol. Chem. 4 (2006) 1572.
[20] D. Parker (Ed.), Macrocyclic Synthesis, A Practical Approach, Oxford University Press, Oxford, UK, 1996.
[21] S.J.A. Pope, A.M. Kenwright, V.A. Boote, S. Faulkner, J. Chem. Soc., Dalton Trans. (2003) 3780.
[22] S.J.A. Pope, A.M. Kenwright, S.L. Heath, S. Faulkner, Chem. Commun. (2003) 1550.
[23] T.-M. Lee, T.-H. Cheng, M.-H. Ou, C.A. Chang, G.-C. Liu, Y.-M. Wang, Magn. Reson. Chem. 42 (2004) 329.
[24] K. Mochizuki, Y. Numata, Inorg. Chem. Commun. 7 (2004) 806.
[25] N.W. Alcock, K.P. Balakrishnan, P. Moore, G.A. Pike, J. Chem. Soc., Dalton Trans. (1987) 889.
[26] J. Paris, C. Gameiro, V. Humblet, P.K. Mohapatra, V. Jacques, J.F. Desreux, Inorg. Chem. 45 (2006) 5092.
[27] L.A. Berben, J.C. Peters, Inorg. Chem. 47 (2008) 11669.
[28] J.L. Sessler, J.W. Sibert, A.K. Burrell, V. Lynch, J.T. Markert, C.L. Wooten, Inorg. Chem. 32 (1993) 4277.
[29] O. Iranzo, T. Elmer, J.P. Richard, J.R. Morrow, Inorg. Chem. 42 (2003) 7737.
[30] J.D. Chartres, A.M. Groth, L.F. Lindoy, M.P. Lowe, G.V. Meehan, J. Chem. Soc., Perkin Trans. 1 (2000) 3444.
[31] B. Boitrel, B. Andrioletti, M. Lakhar, R. Guilard, Tetrahedron Lett. 36 (1995) 4995.
[32] J.D. Chartres, L.F. Lindoy, G.V. Meehan, Tetrahedron 62 (2006) 4173.
[33] G. Royal, V. Dahaoui-Gindrey, S. Dahaoui, A. Tabard, R. Guilard, P. Pullumbri, C. Lecomte, Eur. J. Org. Chem. 63 (1998) 1971.
[34] M. Ramli, M. Dong, L.F. Lindoy, S.V. Smith, J.G. Wilson, J. Heterocycl. Chem. 42 (2005) 77.
[35] P.D. Beer, D. Gao, Chem. Commun. (2000) 443.
[36] P. Bernhardt, J.Y. Kim, Y. Kim, Y.H. Lee, S.C.R. Chow, Chimie 8 (2005) 211.
[37] K. Mochizuki, A. Hasegawa, T. Weyhermüller, Inorg. Chim. Acta 357 (2004) 3245.
[38] M. Salavatti-Niasari, A. Amiri, Trans. Met. Chem. 31 (2006) 157.
[39] (a) D.P. Riley, D.H. Busch, Inorg. Synth. 18 (1978) 36;
(b) A.J. Streeky, D.G. Pillsbury, D.H. Busch, Inorg. Chem. 19 (1980) 3148;
(c) B. Korybut-Daszkiewicz, M. Koima, J.H. Cameron, N. Herron, M.Y. Chavan,

A.J. Jircitano, B.K. Coltrain, G.L. Neer, N.W. Alcock, D.H. Busch, Inorg. Chem. 23 (1984) 903;
(d) N. Hoshino, K.A. Goldsby, D. Busch, Inorg. Chem. 25 (1986) 3000;
(e) N. Hoshino, A. Jircitano, D.H. Busch, Inorg. Chem. 27 (1988) 2292;
(f) J.H. Cameron, M. Kojima, B. Korybut-Daszkiewicz, B.K. Coltrain, T.J. Meade, N.W. Alcock, D.H. Busch, Inorg. Chem. 26 (1987) 427;
(g) D.H. Busch, N.W. Alcock, Chem. Rev. 94 (1994) 585.
[40] B. Korybut-Daszkiewicz, A. Wieckowska, R. Bilewicz, S. Domagala, K. Wozniak, J. Am. Chem. Soc. 123 (2001) 9356.
[41] A. Wieckowska, R. Bilewicz, S. Domagala, K. Wozniak, B. Korybut-Daszkiewicz, A. Tomkiewicz, J. Mrozinski, J. Inorg. Chem. 42 (2003) 5513.
[42] A. Rybka, R. Kolinski, J. Kowalski, R. Szmigielski, S. Domagala, K. Wozniak, A. Wieckowska, R. Bilewicz, B. Korybut-Daszkiewicz, Eur. J. Inorg. Chem. (2007) 172.
[43] Q. Wang, H. Lönnberg, J. Am. Chem. Soc. 128 (2006) 10716.
[44] (a) A. Khan, J. Greenman, S.J. Archibald, Curr. Med. Chem. 14 (2007) 2257;
(b) E. De Clercq, Nat. Rev. Drug Discov. 2 (2003) 581.
[45] E. De Clercq, N. Yamamoto, R. Pauwels, M. Baba, D. Schols, H. Nakashima, J. Balzarini, Z. Debyser, B.A. Murrer, D. Schwartz, D. Thornton, G. Bridger, S. Fricker, G. Henson, M. Abrams, D. Picker, Proc. Natl. Acad. Sci. U.S.A. 89 (1992) 5286.
[46] E.K. Barefield, D. Chueng, C.G. Van Derveer, J. Chem. Soc., Chem. Commun. (1981) 302.
[47] (a) M. Ciampolini, L. Fabbrizzi, A. Perotti, A. Poggi, B. Seghi, F. Zanobini, Inorg. Chem. 26 (1987) 3527;
(b) E. De Clercq, N. Yamamoto, R. Pauwels, J. Balzarini, M. Witvrouw, K. De Vreese, Z. Debyser, B. Rosenwirth, P. Peichl, R. Datema, D. Thornton, R. Skerlj, F. Gaul, S. Padmanabhan, G. Bridger, G. Henson, M. Abrams, Antimicrob. Agents Chemother. 38 (1994) 668.
[48] Monthly Prescribing Reference (December 18, 2008). Mozobil approved for non-Hodgkin's lymphoma and multiple myeloma. Press release. Retrieved on May 12, 2009. http://www.prescribingreference.com/news/showNews/which/MozobilApprovedForNonHodgkinsLymphomaAndMultipleMyeloma121801.
[49] L.O. Gerlach, R.T. Skerlj, G.J. Bridger, T.W. Schwartz, J. Biol. Chem. 276 (2001) 14153.
[50] P. Sadler, S.J. Paisey, Chem. Commun. (2004) 306.
[51] (a) G.J. Bridger, R.T. Skerlj, S. Padmanabhan, S.A. Martellucci, G.W. Henson, M.J. Abrams, H.C. Joao, M. Witvrouw, K. De Vreese, R. Pauwels, E. De Clercq, J. Med. Chem. 39 (1996) 109;
(b) G.J. Bridger, R.T. Skerlj, D. Thornton, S. Padmanabhan, S.A. Martellucci, G.W. Henson, M.J. Abrams, M. Yamamoto, K. De Vreese, R. Pauwels, E. De Clercq, J. Med. Chem. 38 (1995) 366;
(c) J.A. Este, C. Cabrera, E. De Clercq, S. Struyf, J. Van Damme, G. Bridger, R.T. Skerlj, M.J. Abrams, G. Henson, A. Gutierrez, B. Clotet, D. Schols, Mol. Pharm. 55 (1999) 67.
[52] (a) A. Muller, B. Homey, N. Soto, N. Ge, D. Catron, M.E. Buchanan, T. McClanahan, E. Murphy, W. Yuan, S.N. Wagner, J.L. Barrera, A. Mohar, E. Verastegui, A. Zlotnik, Nature 410 (2001) 50;
(b) P. Matthys, S. Hatse, K. Vermeire, A. Wuyts, G. Bridger, G. Henson, E. De Clercq, A. Billiau, D. Schols, J. Immunol. 167 (2001) 4686.
[53] T. Murakami, A.R. Cardones, S.T. Hwang, J. Derm. Sci. 36 (2004) 71.
[54] (a) A.E.I. Proudfoot, Nat. Rev. Immunol. 2 (2002) 106;
(b) J.A. Belperio, M.P. Keane, D.A. Arenberg, C.L. Addison, J.E. Ehlert, M.D. Burdick, R.M. Strieter, J. Leukocyte Biol. 68 (2000) 1;
(c) C.R. Cooper, C.H. Chay, J.D. Gendernalik, H.L. Lee, J. Bhatia, R.S. Taichman, L.K. McCauley, E.T. Keller, K.J. Pienta, Cancer 97 (2003) 739.
[55] A. Ben-Baruch, Breast Cancer Res. 5 (2003) 31.
[56] E. Kimura, Y. Kuramoto, T. Koike, H. Fujioka, M. Kodama, J. Org. Chem. 55 (1990) 42.
[57] Review article: E. Kimura, Top. Curr. Chem. 128 (1985) 113.
[58] (a) G. Schwarzenbach, Helv. Chim. Acta 35 (1952) 2344;
(b) E.L. Simmons, J. Chem. Educ. 56 (1979) 578;
(c) A.E. Martell, R.D. Hancock, R.J. Motekaitis, Coord. Chem. Rev. 133 (1994) 39.
[59] (a) S. Develay, R. Tripier, M. Le Baccon, V. Patinec, G. Serratrice, H. Handel, Dalton Trans. (2005) 3016;
(b) S. Develay, R. Tripier, M. Le Baccon, V. Patinec, G. Serratrice, H. Handel, Dalton Trans. (2006) 3418;
(c) S. Develay, R. Tripier, N. Bernier, M. Le Baccon, V. Patinec, G. Serratrice, H. Handel, Dalton Trans. (2007) 1038;
(d) N. Le Bris, H. Bernard, R. Tripier, H. Handel, Inorg. Chim. Acta 360 (2007) 3026.
[60] D.K. Cabbiness, D.W. Margerum, J. Am. Chem. Soc. 90 (1969) 6450.
[61] A.-S. Delepine, R. Tripier, H. Handel, Org. Biomol. Chem. 6 (2008) 1743.
[62] J. Costa, É. Tóth, L. Helm, A.E. Merbach, Inorg. Chem. 44 (2005) 4747.
[63] J.N. Caille, P. Kien, M. Alard, B. Bonnemain, Am. J. Neuroradiol. 7 (1986) 540.
[64] É. Tóth, L. Helm, A.E. Merbach, in: É. Tóth, A.E. Merbach (Eds.), The Chemistry of Contrast Agents in Medical Magnetic Resonance Imaging, Wiley, Chichester, U.K., 2001.
[65] R. Ruloff, G. van Koten, A.E. Merbach, Chem. Commun. (2004) 842.
[66] É. Tóth, S. Vauthey, D. Pubanz, A.E. Merbach, Inorg. Chem. 35 (1996) 3375.
[67] D.H. Powell, O.M. Ni Dhubughaill, D. Pubanz, L. Helm, Y.S. Lebedev, W. Schlaepfer, A.E. Merbach, J. Am. Chem. Soc. 118 (1996) 9333.
[68] J. Carvalho, A.D. Watson, J.D. Fellman, M.D. Koo, US Patent 5,650,133 (1988).
[69] V. Comblin, D. Gilsoul, M. Hermann, V. Humblet, V. Jacques, M. Meshabi, C. Sauvage, J.F. Desreux, Coord. Chem. Rev. 185–186 (1999) 451.
[70] A. Mishra, P. Fouskova, G. Angelovski, E. Balogh, A.K. Mishra, N.K. Logothetis, É. Tóth, Inorg. Chem. 47 (2008) 1370.
[71] (a) M. Massimini, F. Amzica, J. Neurophysiol. 85 (2001) 1346;
(b) I.A. Silver, M. Erecinska, J. Gen. Physiol. 95 (1990) 837.
[72] (a) A. Beeby, S. Faulkner, Chem. Phys. Lett. 266 (1997) 116;
(b) A. Beeby, R.S. Dickins, S. Faulkner, Chem. Commun. 13 (1997) 1401;
(c) P.G. Sammes, G. Yahogliou, Natl. Prod. Rep. (1996) 1;
(d) L. Charbonniere, R. Ziessel, M. Guardigli, A. Roda, N. Sabbatini, M. Cesarion, J. Am. Chem. Soc. 123 (2001) 2436.
[73] (a) S. Faulkner, S.J.A. Pope, J. Am. Chem. Soc. 125 (2003) 10526;
(b) S.J.A. Pope, A.M. Kenwright, V.A. Boote, S. Faulkner, Dalton Trans. (2003) 3780.
[74] S. Aoki, M. Zulkefeli, M. Shiro, M. Kohsako, K. Takeda, E. Kimura, J. Am. Chem. Soc. 127 (2005) 9129.
[75] (a) G.J. Kavarno, N.J. Turro, Chem. Rev. 86 (1986) 401;
(b) J.-P. Sauvage, J.-P. Colin, J.-C. Chambron, S. Guillerez, C. Coudret, Chem. Rev. 94 (1994) 993.
[76] C.P. Mathews, E.K. van Hold, Biochemistry, The Benamin/Cummings Publishing Co. Inc., Redwood City, CA, 1990.
[77] (a) D. Parker, Chem. Soc. Rev. 19 (1990) 271;
(b) C.J. Anderson, M.J. Welch, Chem. Rev. 99 (1999) 2219.
[78] M. Ramli, S.V. Smith, L.F. Lindoy, Bioconjugate Chem. 20 (2009) 868.
[79] S.J. Archibald, E.A. Lewis, T.J. Hubin, EP Patent 1,765,826 B1 (2008).
[80] S.J. Archibald, T.J. Hubin, unpublished results.
[81] T. Koike, M. Takashige, E. Kimura, H. Fujioka, M. Shiro, Chem. Eur. J. 2 (1996) 617.
[82] H. Fujioka, T. Koike, N. Yamada, E. Kimura, Heterocycles 42 (1996) 775.
[83] (a) J.E. Coleman, Annu. Rev. Biophys. Biomol. Struct. 21 (1992) 441;
(b) E.E. Kim, H.W. Wyckoff, J. Mol. Biol. 218 (1991) 449.
[84] E. Kimura, S. Aoki, T. Koike, M. Shiro, J. Am. Chem. Soc. 119 (1997) 3068.
[85] M. Shionoya, E. Kimura, M. Shiro, J. Am. Chem. Soc. 115 (1993) 6730.
[86] S. Aoki, C. Sugimura, E. Kimura, J. Am. Chem. Soc. 120 (1998) 10094.
[87] E. Kimura, M. Kikuchi, H. Kitamura, T. Koike, Chem. Eur. J. 5 (5) (1999) 3113.
[88] (a) J.C. Martin (Ed.), Nucleotide Analogues as Antiviral Agents, American Chemical Society, Washington, DC, 1989.;
(b) T.C. Merigan Jr., J.G. Bartlett, D. Bolognesi, Textbook of AIDS Medicine, 2nd ed., Williams & Williams, Baltimore, 1999;
(c) E. De Clercq, J. Med. Chem. 38 (1995) 2491.
[89] E. Kimura, T. Koiko, J. Chem. Soc., Chem. Commun. (1998) 1495.
[90] S. Aoki, E. Kimura, J. Am. Chem. Soc. 122 (2000) 4542.
[91] E. Kikuta, S. Aoki, E. Kimura, J. Biol. Inorg. Chem. 7 (2002) 473.
[92] M.W. van Dyke, R.P. Hertzberg, P.B. Dervan, Proc. Natl. Acad. Sci. U.S.A. 79 (1982) 5470.
[93] (a) C. Bazzicalupi, A. Bencini, E. Berni, C. Giorgi, S. Maoggi, B. Valtancoli, Dalton Trans. (2003) 3574;
(b) A. Bencini, E. Berni, A. Bianchi, C. Giorgi, B. Valtancoli, D.K. Chand, H.-J. Schneider, Dalton Trans. (2003) 793.
[94] (a) W.N. Lipscomb, M. Strater, Chem. Rev. 96 (1996) 2375;
(b) D.E. Wilcox, Chem. Rev. 96 (1996) 2435;
(c) N. Strater, W.M. Lipscomb, T. Klabunde, B. Krebs, Angew. Chem., Int. Ed. Engl. 35 (1996) 2024.
[95] T. Koike, E. Kimura, J. Am. Chem. Soc. 113 (1991) 8935.
[96] (a) O. Iranzo, A.Y. Kovalevsky, J.R. Morrow, J.P. Richard, J. Am. Chem. Soc. 125 (2003) 1988;
(b) M.-Y. Yang, J.P. Richard, J.R. Morrow, Chem. Commun. (2003) 2832;
(c) O. Iranzo, J.P. Richard, J.R. Morrow, Inorg. Chem. 43 (2004) 1743;
(d) M.-Y. Yang, O. Iranzo, J.P. Richard, J.R. Morrow, J. Am. Chem. Soc. 127 (2005) 1064;
(e) A. O'Donoghue, S.Y. Pyun, M.-Y. Yang, J.R. Morrow, J.P. Richard, J. Am. Chem. Soc. 128 (2006) 1615.
[97] F.H. Fry, B. Moubaraki, K.S. Murray, L. Spicca, M. Warren, B.W. Skelton, A.H. White, Dalton Trans. (2003) 866.
[98] R.L. Schowen, Prog. Phys. Org. Chem. 9 (1972) 275.
[99] (a) R.S. Brown, A.A. Neverov, Adv. Phys. Org. Chem. 42 (2007) 271;
(b) A.A. Neverov, Z.-L. Lu, C.I. Maxwell, M.F. Mohamed, C.J. White, J.S.W. Tsang, R.S. Brown, J. Am. Chem. Soc. 128 (2006) 16398;
(c) S.E. Bunn, C.T. Liu, Z.-L. Lu, A.A. Neverov, R.S. Brown, J. Am. Chem. Soc. 129 (2007) 16238;
(d) Z.-L. Lu, C.T. Liu, A.A. Neverov, R.S. Brown, J. Am. Chem. Soc. 129 (2007) 11642;
(e) A.A. Neverov, C.T. Liu, S.E. Bunn, D. Edwards, C.J. White, S.A. Melnychuk, R.S. Brown, J. Am. Chem. Soc. 130 (2008) 6639.
[100] (a) W.W. Cleland, P.A. Frey, J.A. Gerlt, J. Biol. Chem. 273 (1998) 25529;
(b) R.M. Czerwinski, T.K. Harris, M.A. Massiah, A.S. Mildvan, C.P. Whitman, Biochemistry 40 (2001) 1984;
(c) F. Plow, D. Kowlessur, J.P.G. Malthouse, G.W. Mellor, M.J. Hartshorn, H.P. Pinitglang, C.M. Topham, E.W. Thomas, C. Verma, K. Brocklehurst, J. Mol. Biol. 257 (1996) 1088;
(d) R.E. Cachau, E.B. Garcia-Moreno, J. Mol. Biol. 255 (1996) 340;
(e) R. Kanski, C.J. Murray, Tetrahedron Lett. 34 (1993) 2263.
[101] J. Kim, H. Lim, Bull. Korean Chem. Soc. 20 (1999) 491.
[102] C.T. Liu, A.A. Neverov, R.S. Brown, J. Am. Chem. Soc. 130 (2008) 13870.
[103] C. Vichard, T.A. Kaden, Inorg. Chim. Acta 337 (2002) 173.

[104] (a) M. Subat, K. Woinaroschy, S. Anthofer, B. Malterer, B. Konig, Inorg. Chem. 46 (2007) 4336;
(b) M. Subat, K. Woinaroschy, C. Gerstl, B. Sarkar, W. Kaim, B. Konig, Inorg. Chem. 47 (2008) 4661.
[105] C.E. Yoo, P.S. Chae, J.E. Kim, E.J. Jeong, J. Suh, J. Am. Chem. Soc. 125 (2003) 14580.
[106] S.J. Brudenell, L. Spicca, A.M. Bond, G.D. Fallon, D.C. Hockless, G. Lazarev, P.J. Mahon, E.R.T. Tiekink, Inorg. Chem. 39 (2000) 881.
[107] (a) R. Hage, J.E. Iburg, J. Kerschner, J.H. Koek, E.L.M. Lempers, R.J. Martens, U.S. Racherla, S.W. Russell, T. Swarthoff, M.R.P. van Vliet, J.B. Warnaar, L. van der Wolf, B. Krljen, Science 369 (1994) 637;
(b) D.E. de Vos, T. Ben, J. Organomet. Chem. 520 (1996) 195;
(c) C. Zondervan, R. Hage, B.L. Ferigna, Chem. Commun. (1997) 419;
(d) K. Wieghardt, U. Bossek, D. Ventur, J. Weiss, Chem. Commun. (1985) 347;
(e) K. Wieghardt, U. Bossek, J. Bonvoisin, P. Beauvillain, J.J. Girerd, B. Nuber, J. Weiss, J. Heinze, Angew. Chem., Int. Ed. Engl. 25 (1986) 1030;
(f) K. Wieghardt, I. Tolksdorf, W. Herrmann, Inorg. Chem. 24 (1985) 1230;
(g) K. Wieghardt, U. Bossek, L. Zsolnai, G. Huttner, G. Blondin, J.-J. Girerd, F. Babonneau, Chem. Commun. (1987) 651;
(h) K. Wieghardt, E. Schoffman, B. Nuber, J. Weiss, Inorg. Chem. 25 (1986) 4877.
[108] (a) M. Beley, J.P. Collin, R. Ruppert, J.P. Sauvage, J. Chem. Soc., Chem. Commun. (1984) 1315;
(b) M. Beley, J.P. Collin, R. Ruppert, J.P. Sauvage, J. Am. Chem. Soc. 108 (1986) 7461;
(c) G.B. Balazs, F.C. Anson, J. Electroanal. Chem. 322 (1992) 325;
(d) G.B. Balazs, F.C. Anson, J. Electroanal. Chem. 361 (1993) 149.
[109] C. de Alwis, J.A. Crayston, T. Cromie, T. Eisenblatter, R.W. Hay, Y.D. Lampeka, L.V. Tsymbal, Electrochim. Acta 45 (2000) 2061.
[110] E. Kimura, T. Koike, Y. Inouye, Perspect. Bioinorg. Chem. 4 (1999) 145.
[111] X. Liang, P.J. Sadler, Chem. Soc. Rev. 33 (2004) 246.
[112] (a) X. Liang, J.A. Parkinson, M. Weishaupl, G.O. Gould, S.J. Paisey, H. Park, T.M. Hunter, C.A. Blindauer, S. Parsons, P.J. Sadler, J. Am. Chem. Soc. 124 (2002) 9105;
(b) X. Liang, M. Weishaupl, J.A. Parkinson, S. Parsons, P.A. McGregor, P.J. Sadler, Chem. Eur. J. 9 (2003) 4709.
[113] L.O. Gerlach, J.S. Jakobsen, K.P. Jensen, M.R. Rosenkilde, R.T. Skerlj, U. Ryde, G.J. Bridger, T.W. Schwartz, Biochemistry 42 (2003) 710.
[114] M.M. Rosenkilde, L.O. Gerlach, J.S. Jakobsen, R.T. Skerlj, G.J. Bridger, T.W. Schwartz, J. Biol. Chem. 279 (2004) 3033.
[115] (a) G. McRobbie, G.C. Valks, C.J. Empson, A. Khan, J.D. Silversides, C. Pannecouque, E. De Clercq, S.G. Fiddy, A.J. Bridgeman, N.A. Young, S.J. Archibald, Dalton Trans. (2007) 5008;
(b) A. Khan, MSc Thesis, University of Hull, Hull, UK, 2006;
(c) E.A. Lewis, R.W. Boyle, S.J. Archibald, Chem. Commun. (2004) 2212.
[116] T.J. Hubin, Coord. Chem. Rev. 241 (2003) 27.